$b \to s\mu\mu$ 理論

三島 智 (埼玉医大)

研究会「フレーバーアノマリーの現状とBファクトリーの未来」，2024年 8月6-7日

$b \to s$ anomalies

- FCNC $b \to s\mu\mu$ processes offer sensitive probes for NP due to suppression in SM.

- In particular, $B \to K^{(*)}\mu\mu$ have been attracting a lot of attention because of observed ***anomalies***.

- Lepton-flavor-universality (LFU) ratios $R_{K^{(*)}}$, reported by LHC on Dec. 2022, are **consistent with SM**.

LHCb, 1512.04442

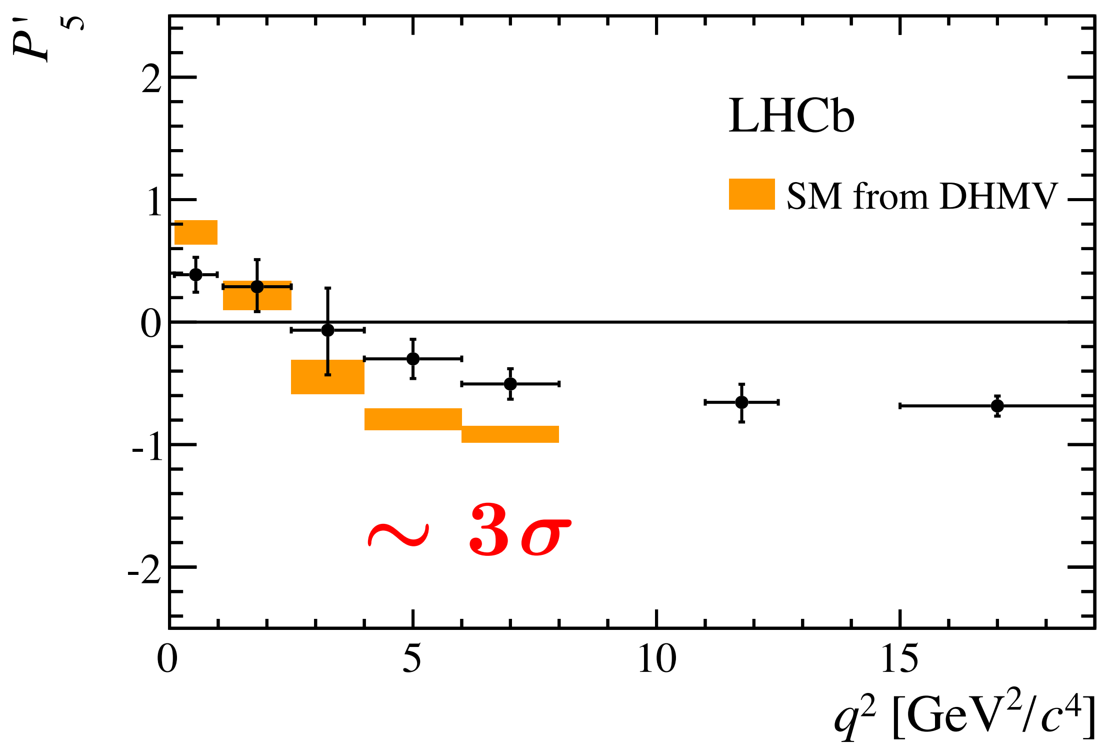

LHCb, 2212.09152; 2212.09153

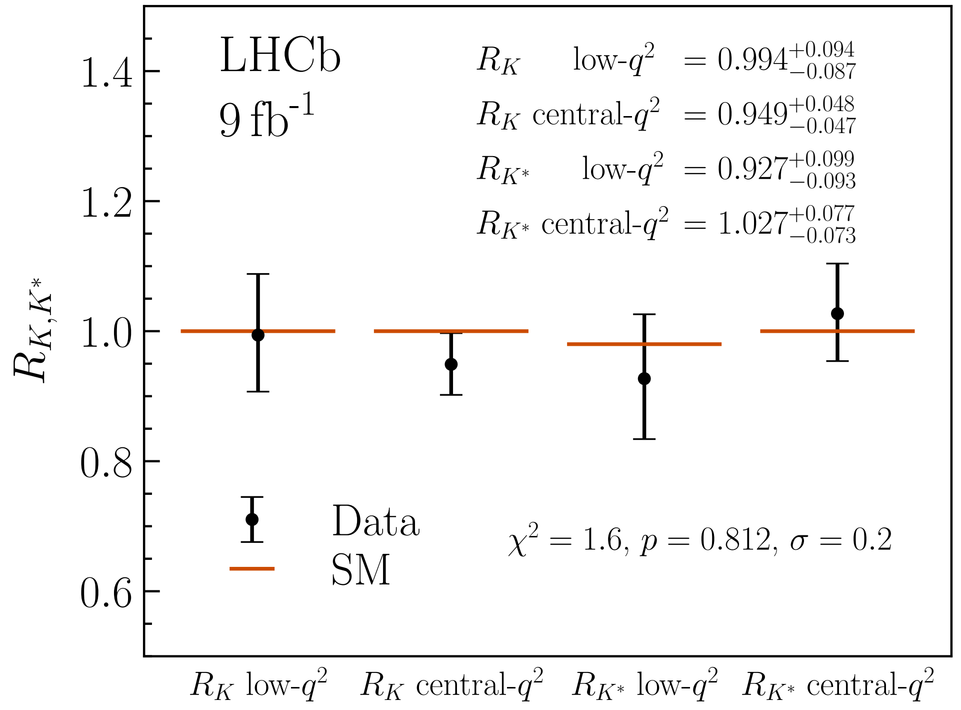

Outline

- Theoretical framework
- Non-local charm loop
- Global fit and NP interpretation
- Summary

Theoretical framework

Low-energy effective theory

- Flavor observables are calculated with effective field theory (EFT).

$$\mathcal{L}_{\mathrm{eff}} = \sum_i \mathcal{C}_i(\mu)\mathcal{O}_i(\mu)$$

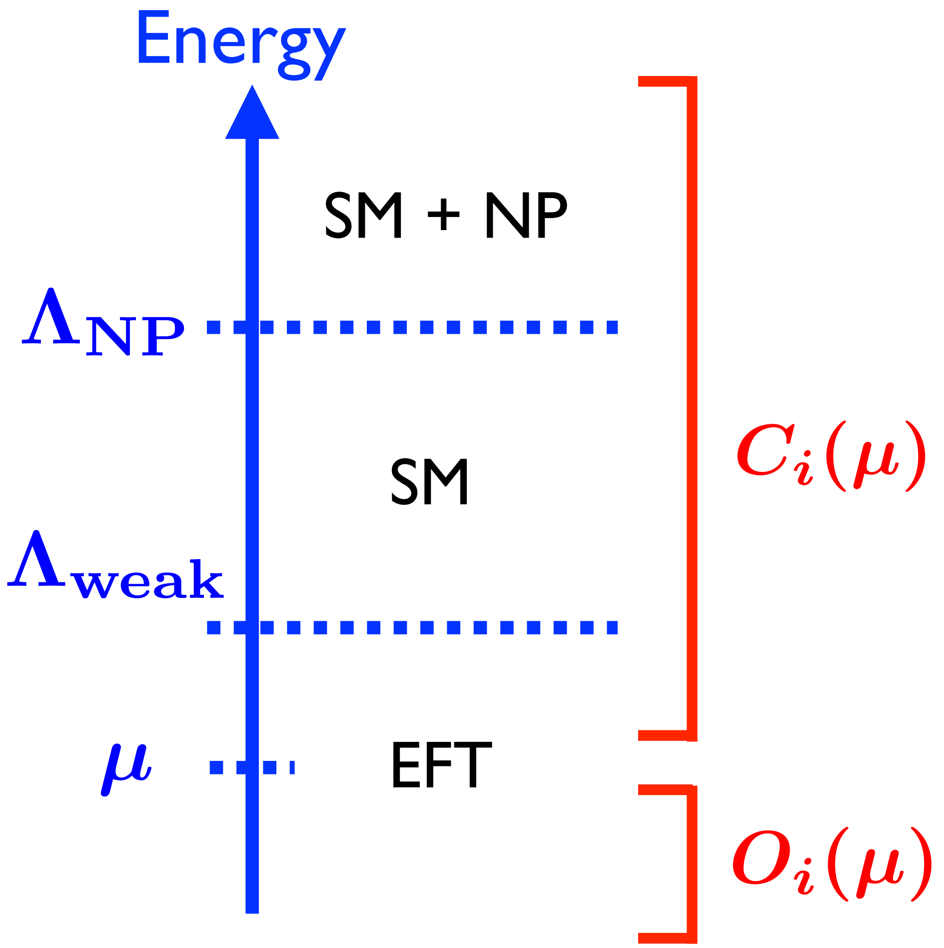

- Dominant contributions to $B \to K^{(*)}\mu^+\mu^-$:

$$\mathcal{O}_9 \sim \left(\bar{s}\gamma^\mu P_L b\right)\left(\bar{\ell}\gamma_\mu \ell\right)$$

$$\mathcal{O}_{10} \sim \left(\bar{s}\gamma^\mu P_L b\right)\left(\bar{\ell}\gamma_\mu\gamma_5 \ell\right)$$

$$\mathcal{O}_7 \sim m_b\left(\bar{s}\sigma^{\mu\nu} P_R b\right)F_{\mu\nu}$$

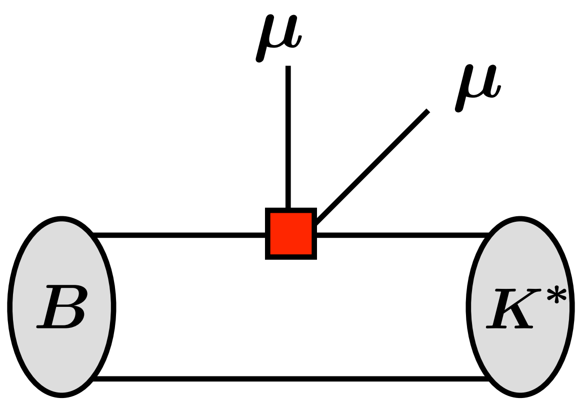

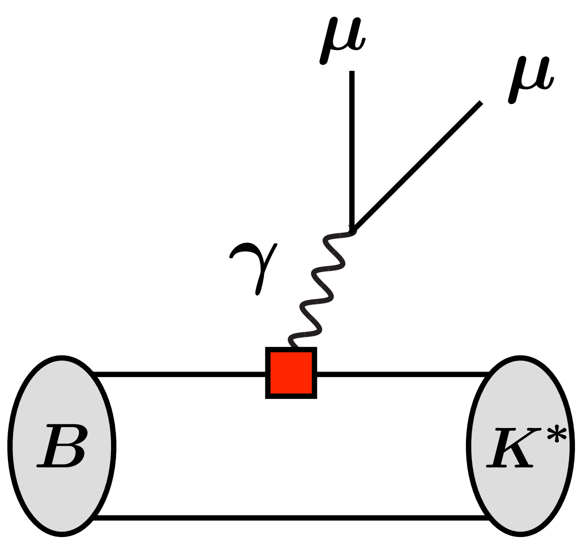

$$\mathcal{C}_9^{\mathrm{SM}}(m_b) \sim 4.1$$

$$\mathcal{C}_{10}^{\mathrm{SM}}(m_b) \sim -4.2$$

$B \to K^{(*)}\mu^+\mu^-$

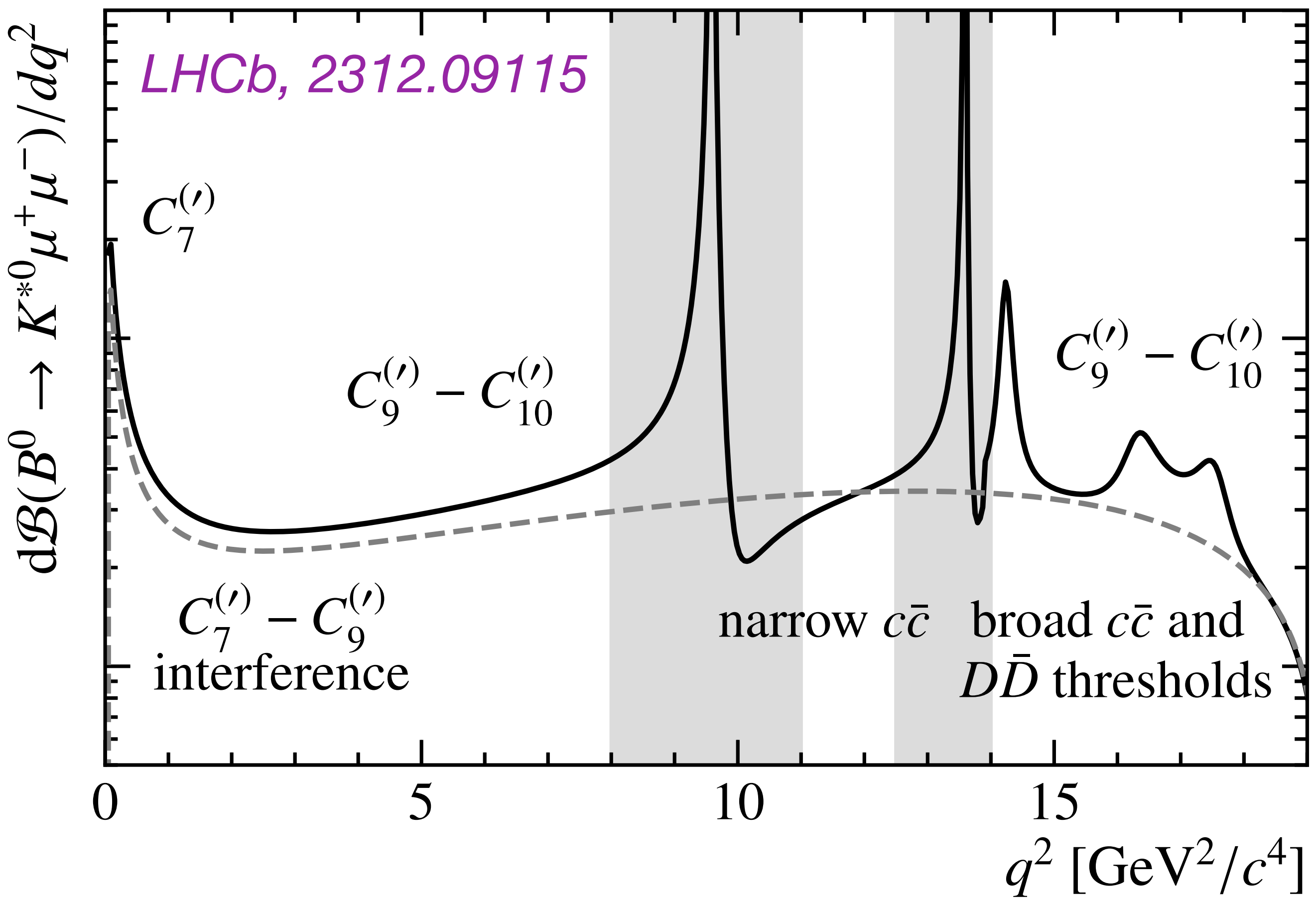

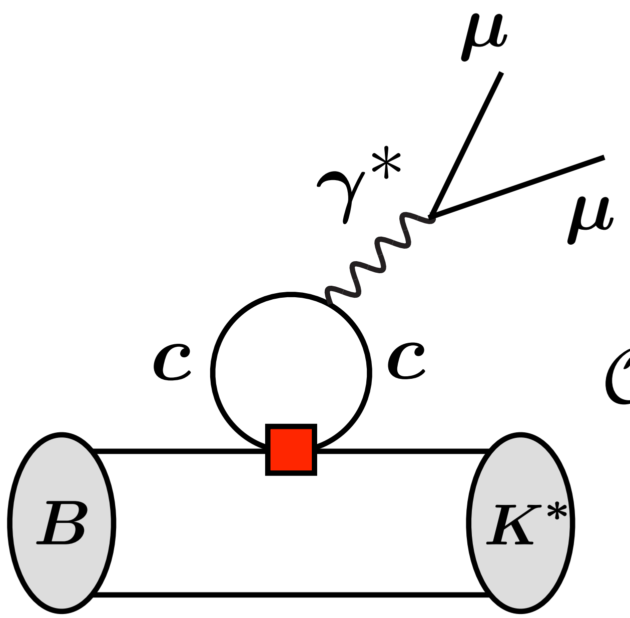

$\mathcal{O}_2 \sim (\bar{c}\gamma^\mu P_L b)(\bar{s}\gamma_\mu P_L c)$

- Dominant coefficients in each region are shown in plot.
- Gray regions are dominated by $c\bar{c}$ resonant contributions.

$$B \to J/\psi K^{(*)} \;\; \& \;\; B \to \psi(2S) K^{(*)}$$

- **How to calculate or estimate magnitude and phase of resonant amplitude?**
  - I will explain recent studies later.

Form factors

- Theoretical calc's of $B \to K^{(*)}\mu\mu$ decay amplitudes also suffer from uncertainties in $B \to K^{(*)}$ form factors (FFs).
- FFs are calculated with non-perturbative methods.
- Lattice QCD is applicable in high-q^2 (low-recoil of K^*), while light-cone sum rules (LCSR) is in low-q^2 (large recoil of K^*).
- Recent developments:
  - Lattice result for $B \to K$ in full q^2 range. *Parrott et al. [HPQCD], 2207.12468; 2207.13371*
  - Updates of LCSR calculations for $B \to K^*$ in low q^2.

Gubernari et al., 2011.09813; 2305.06301

$B \to K\mu^+\mu^-$

- B($B\to K\mu\mu$) : Reduction of uncertainty without significant shifts in central values. **Tensions in low q^2 increases up to 4σ level.** *Parrott et al. [HPQCD], 2207.12468; 2207.13371*

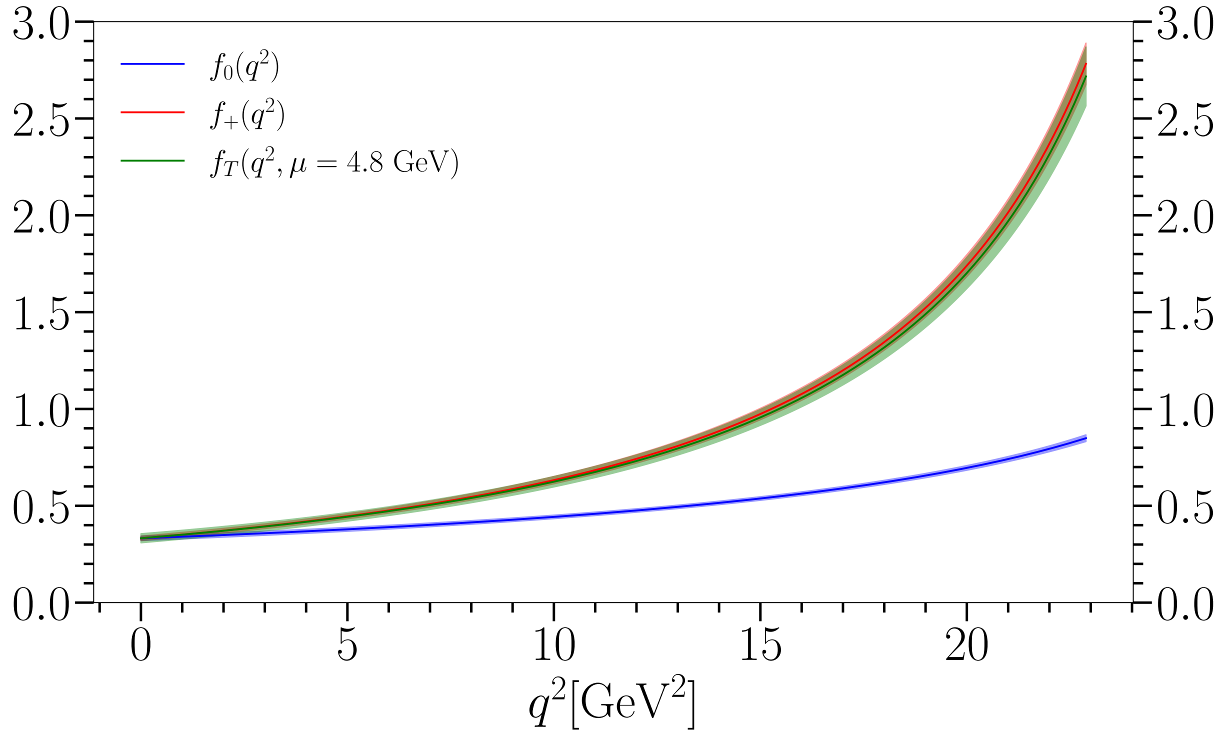

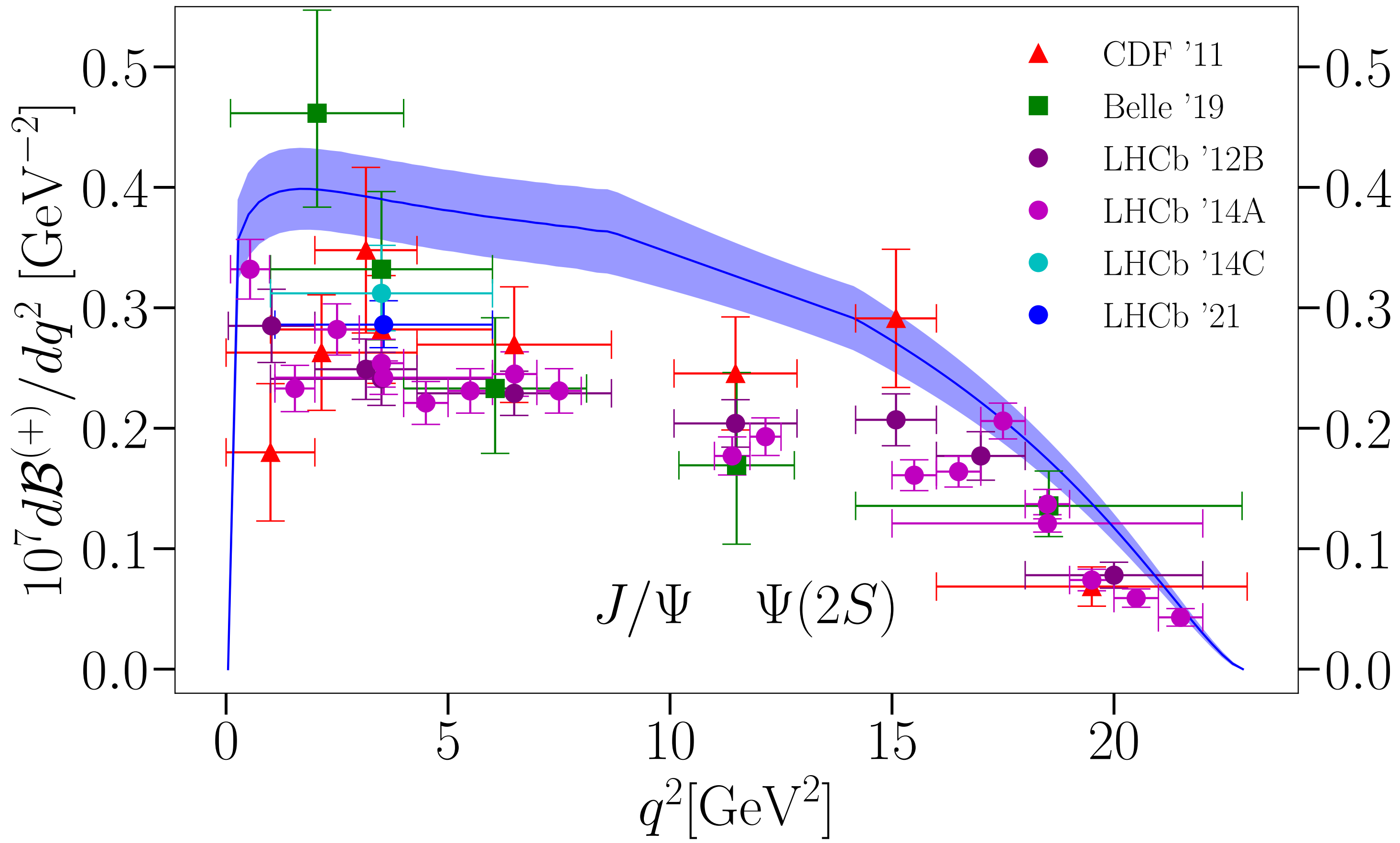

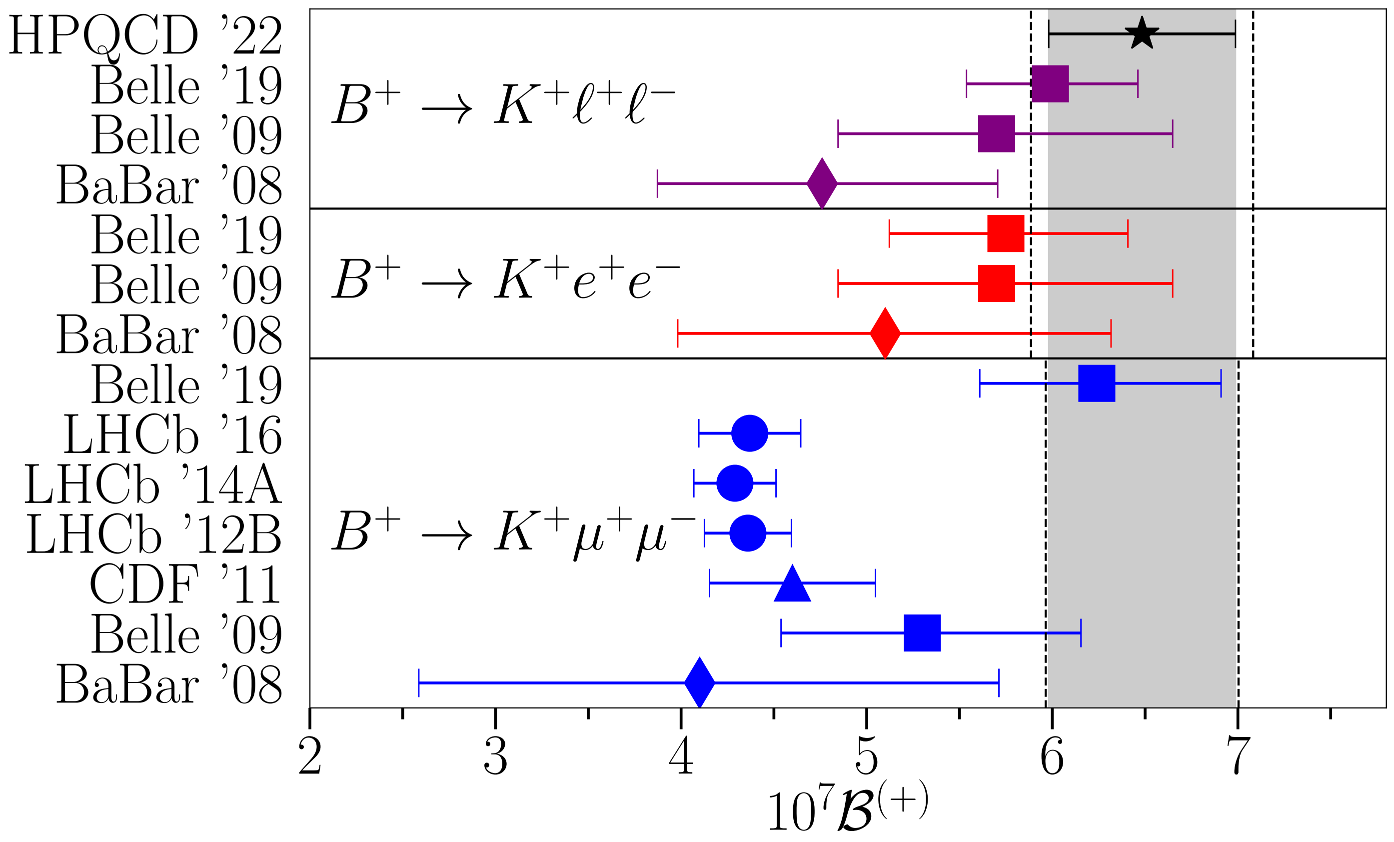

$B \to K^* \mu^+ \mu^-$

- B($B \to K^*\mu\mu$) in low q^2: Uncertainties are reduced by half with lower central values, **compatible with data**.

Gubernari et al., 2206.03797

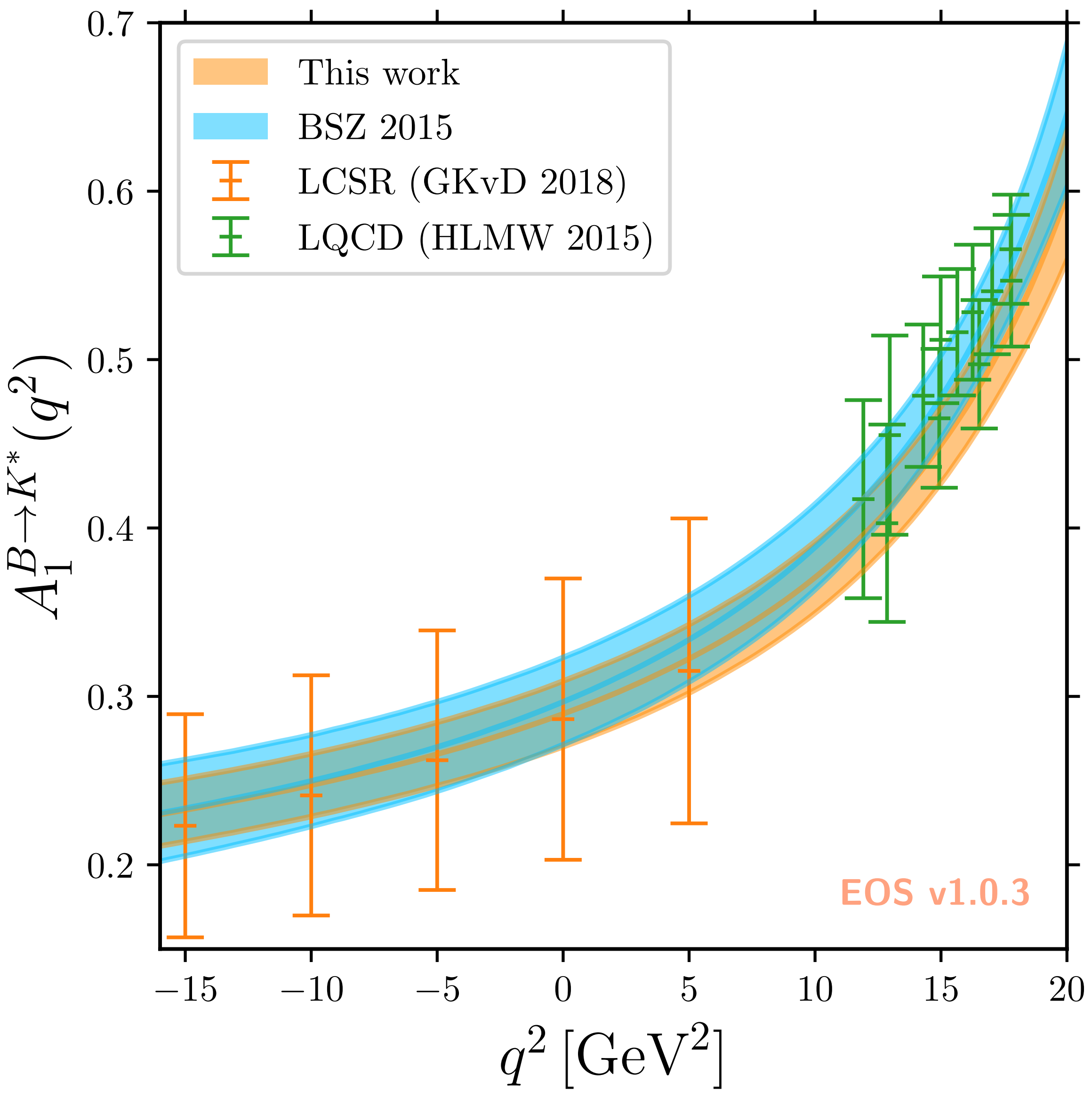

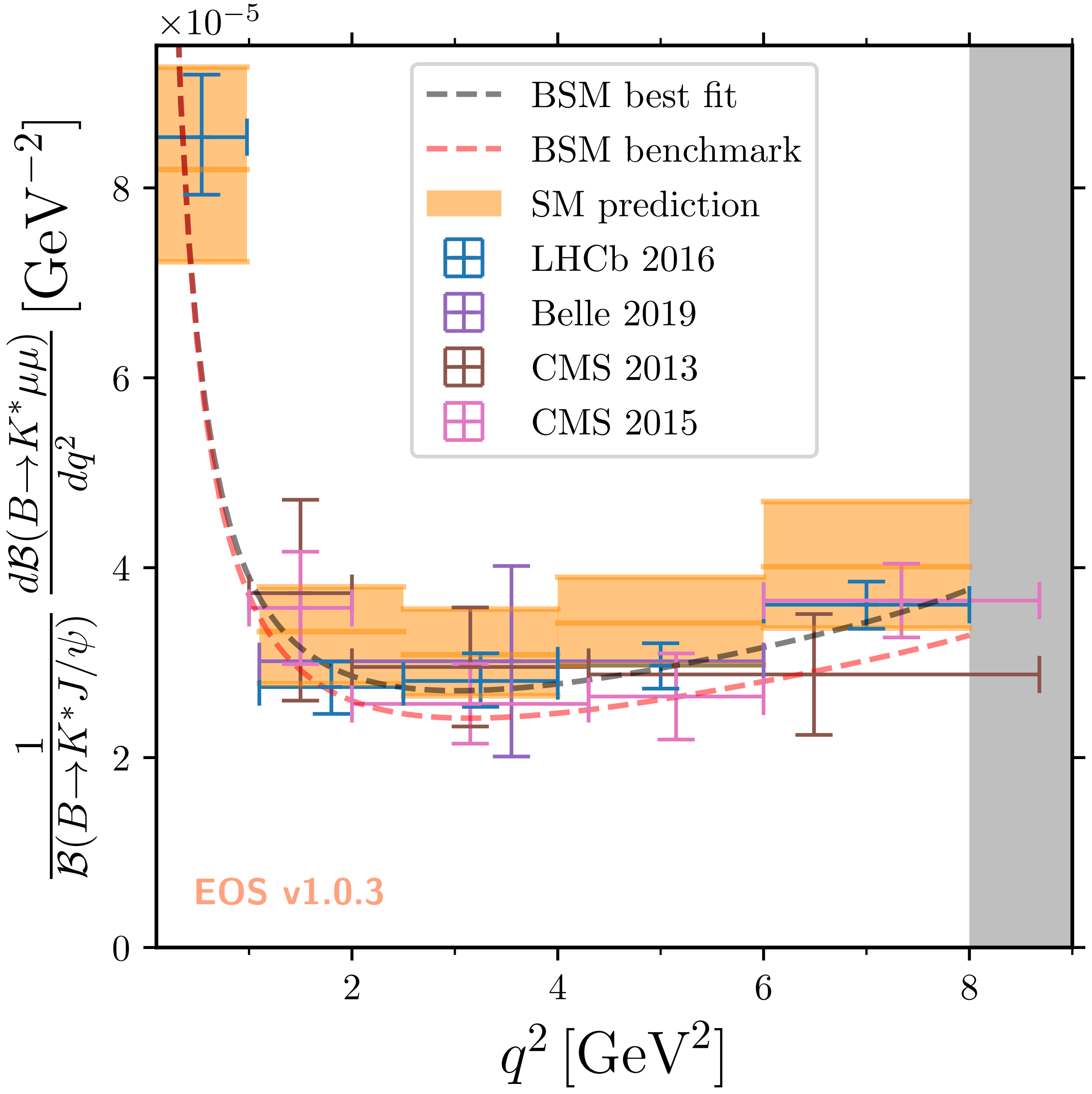

Optimized observables

- SM predictions for Br's are affected by uncertainties from FFs, etc.
- Optimized angular observables, such as P'_5, are constructed such that FFs cancel in ratios at LO in $1/m_b$ and α_s.
- P'_5 in low q^2: **Tensions decreases to 2σ level,** since central values shifts slightly towards data. *Gubernari et al., 2206.03797*
- Both **Br's and P'_5 suffer from hadronic uncertainties through charm loop**, which do not allow us to draw definite conclusions.

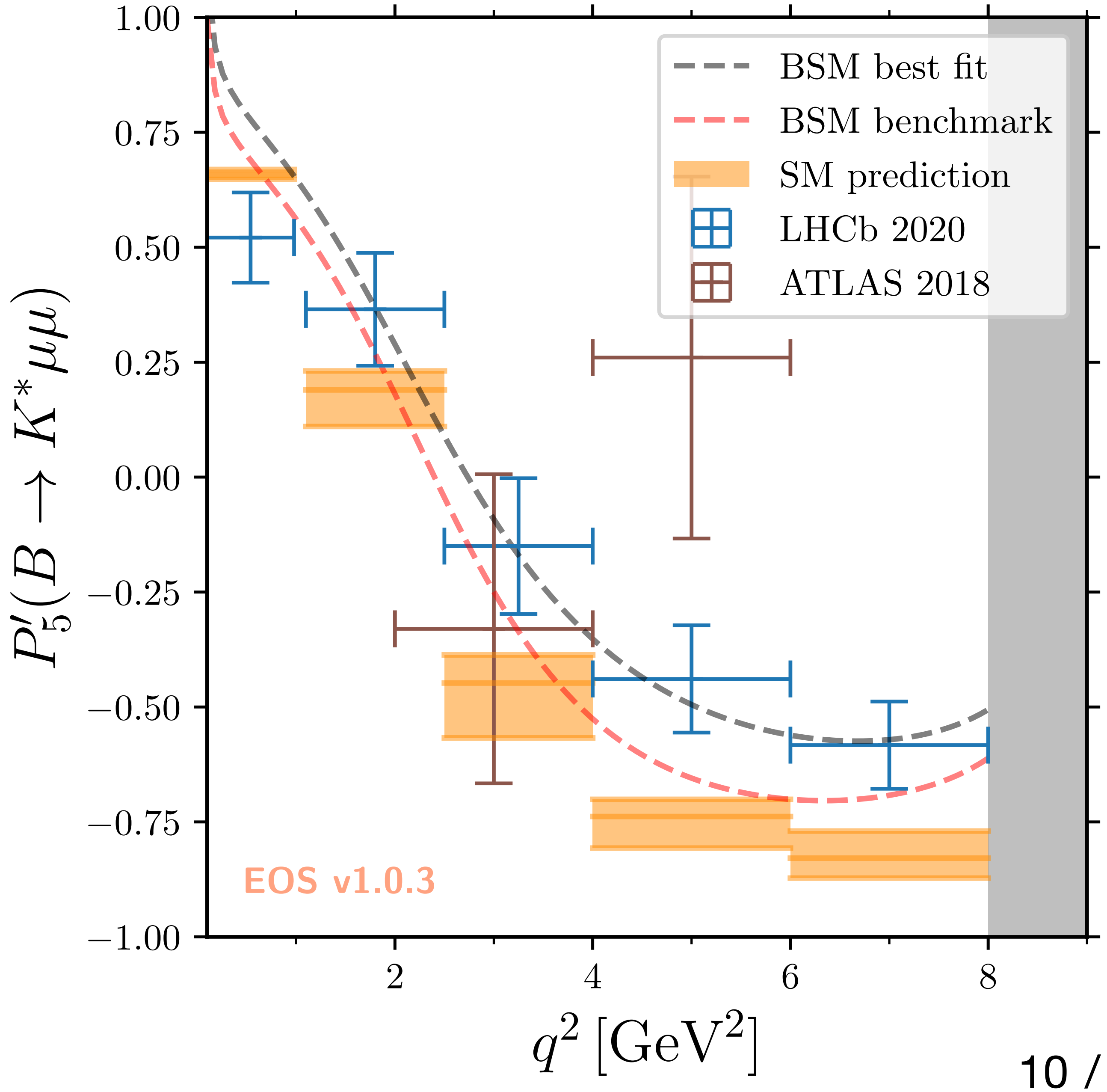

Non-local charm loop

Non-local matrix elements

- Amplitudes are expressed with hadronic matrix elements:

$$\mathcal{A}(\bar{B} \to M\ell^+\ell^-) = \frac{G_F\,\alpha\,V_{ts}^* V_{tb}}{\sqrt{2}\pi}\left[(C_9\,L_V^\mu + C_{10}\,L_A^\mu)\,\mathcal{F}_\mu^{B\to M} - \frac{L_V^\mu}{q^2}\left\{2im_b C_7\,\mathcal{F}_{T,\mu}^{B\to M} + 16\pi^2\mathcal{H}_\mu^{B\to M}\right\}\right]$$

$$L_{V(A)}^\mu \equiv \bar{u}_\ell(q_1)\gamma^\mu(\gamma_5)v_\ell(q_2)$$

  - Local matrix elements:

$$\mathcal{F}_\mu^{B\to M}(k,q) \equiv \langle M(k)|\bar{s}\gamma_\mu P_L\,b|\bar{B}(q+k)\rangle\ ,$$

$$\mathcal{F}_{T,\mu}^{B\to M}(k,q) \equiv \langle M(k)|\bar{s}\sigma_{\mu\nu}q^\nu P_R\,b|\bar{B}(q+k)\rangle\ ,$$

  - Non-local matrix elements:

$$\mathcal{H}_\mu^{B\to M}(k,q) \equiv i\int d^4x\,e^{iq\cdot x}\,\langle M(k)|T\{j_\mu^{\mathrm{em}}(x),(C_1\mathcal{O}_1 + C_2\mathcal{O}_2)(0)\}|\bar{B}(q+k)\rangle\ ,$$

$$j_\mu^{\mathrm{em}} = \sum_q Q_q\ \bar{q}\gamma_\mu q\ \text{ with }\ q = \{u,d,s,c,b\}$$

- Non-local contributions affect determinations of C_7 & C_9 from data.

Charm loop

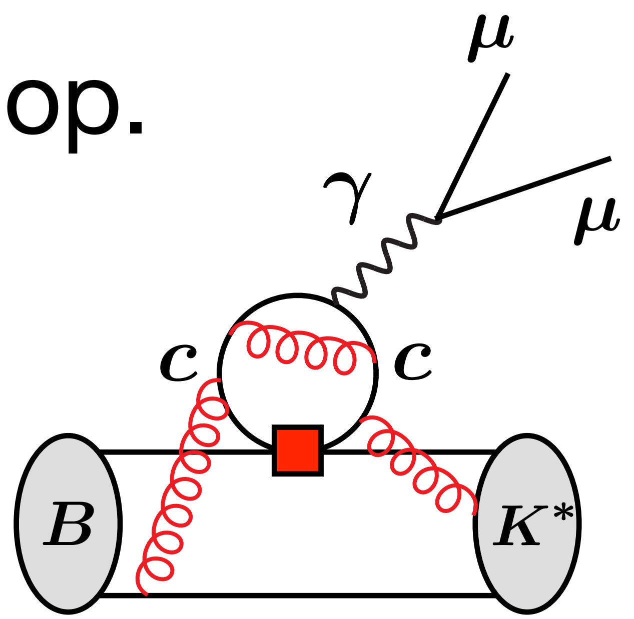

- ✦ Dominant non-local contribution comes from charm loop.
- ✦ **Charm loop is difficult to calculate reliably from first principles.**
- ✦ Calculations & estimations of charm loop:
  - ▸ Light-cone sum rules (LCSR) for negative q^2. *Khodjamirian et al., 1006.4945; Gubernari et al., 2011.09813*
  - ▸ q^2 dep. is parameterized by different ways: *model uncertainty?*
    - ▸ z-expansion with analyticity, *Bobeth et al., 1707.07305*
    - ▸ dispersion relations, *Khodjamirian et al., 1006.4945; 1211.0234; Lyon &Zwicky, 1406.0566; Blake et al., 1709.03921; Cornella et al., 2001.04470; Bordone et al., 2401.18007*
    - ▸ more phenomenological approaches. *Ciuchini et al., 1512.07157; 2212.10516*

LCSR

- Light-cone OPE is carried out for negative q^2 to ensure rapid convergence.

- Leading-power operators coincide with ones in local OPE, *i.e.*, their matrix elements can be expressed in terms of local FFs.

- Next-to-leading power contributions involve operators with insertion of a single soft-gluon field. Their matrix elements are calculated with three-particle *B*-meson light-cone distribution amplitudes (*B*-LCDAs).

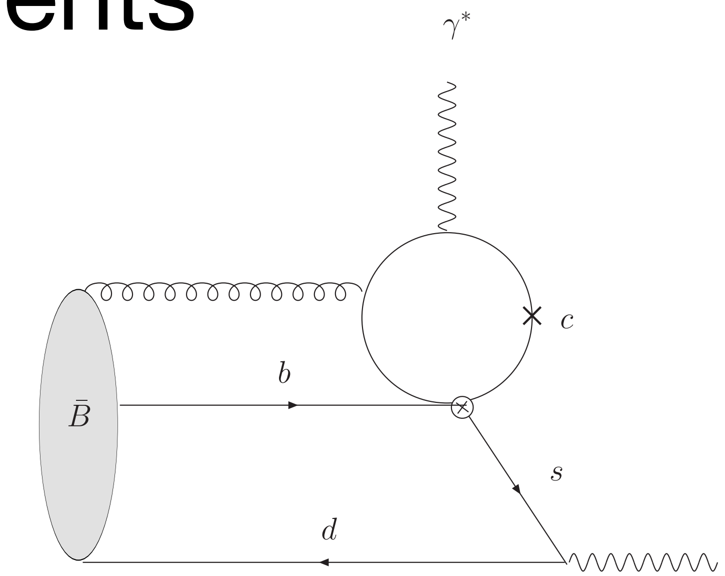

- First calculation was done in 2010. *Khodjamirian et al., 1006.4945*

LCSR (cont'd)

Gubernari et al., 2011.09813

- Next-to-leading power contributions were recalculated in 2020.
- Previous calculation used an incomplete set of B-LCDAs.
- New results are ***two order of magnitude smaller*** than previous one due to cancellations arising from inclusion of full B-LCDAs.
- LCSR results have to be extrapolated to higher values of q^2, in a model-dependent way.
- New LCSR results support that charm loop is not the source of anomalies.

Gubernari et al., 2206.03797

z-expansion with analyticity

- Non-local amplitudes are parametrized with *z*:

outer function that ensures correct kinematic dependencies, e.g.,

$$\mathcal{H}_0(q^2=0)=0,$$

$$\mathcal{H}_\lambda(z) = \frac{1-z\,z_{J/\psi}}{z-z_{J/\psi}}\,\frac{1-z\,z_{\psi(2S)}}{z-z_{\psi(2S)}}\,\hat{\mathcal{H}}_\lambda(z), \qquad \hat{\mathcal{H}}_\lambda(z)=\phi_\lambda^{-1}(z)\sum_k a_{\lambda,k}z^k$$

$$q^2 \mapsto z(q^2) \equiv \frac{\sqrt{t_+-q^2}-\sqrt{t_+-t_0}}{\sqrt{t_+-q^2}+\sqrt{t_+-t_0}}$$

$$t_+ = 4M_D^2$$

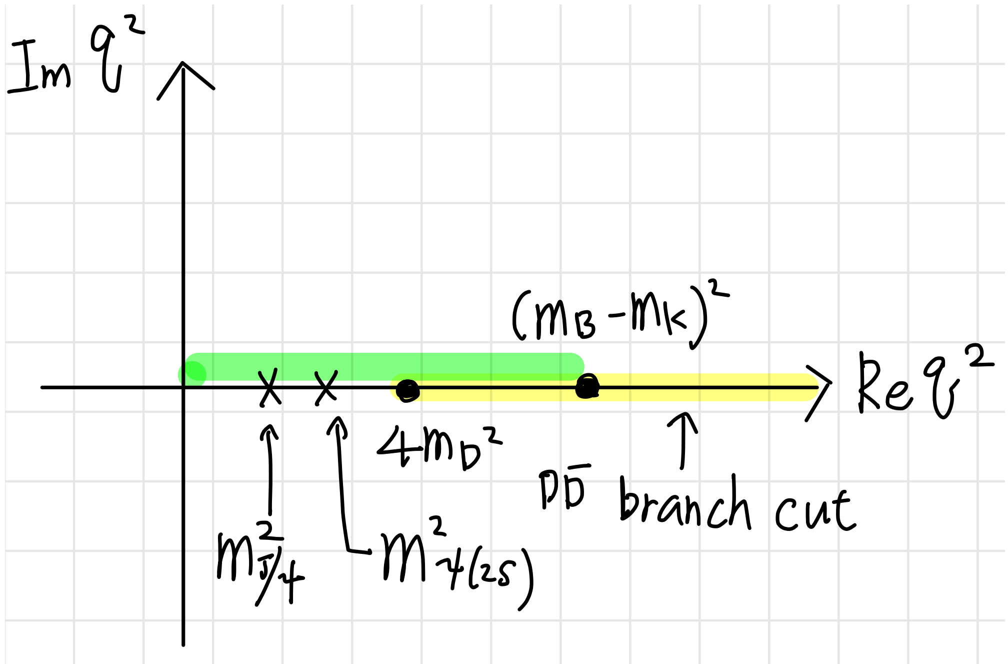

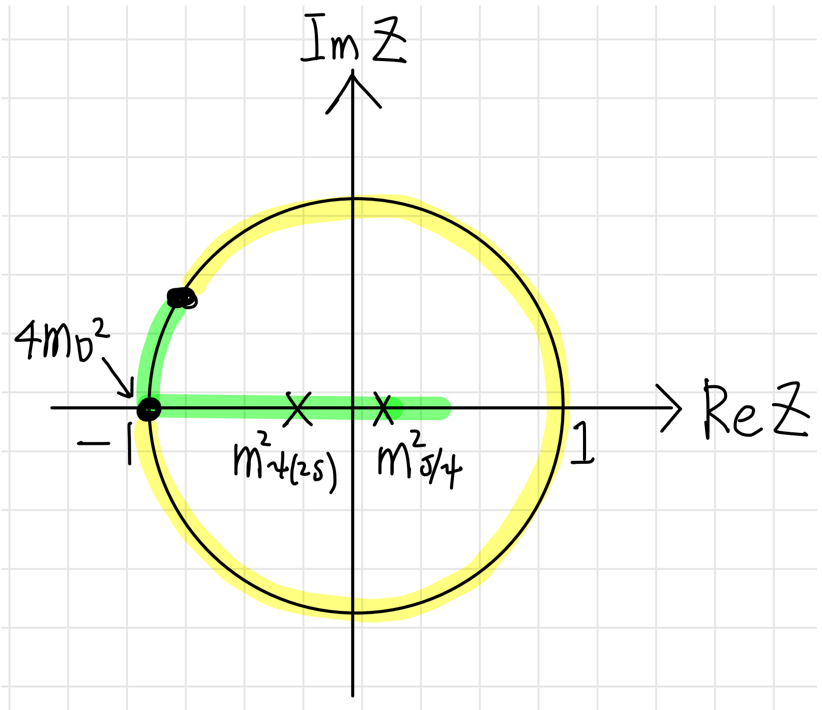

- Branch cut in q^2 plane is mapped onto $|z|=1$ circle.
- This works for q^2 below branch cut.

truncation error? *model uncertainty?*

Bobeth et al., 1707.07305; Gubernari et al., 2011.09813

z-expansion with analyticity (LHCb)

- LHCb determined both SD FFs and LD charm loop from fit to data.

$$F_i(q^2) = \frac{1}{1 - q^2/m_{R,i}^2} \sum_{k=0}^{2} \alpha_{i,k}[z(q^2) - z(0)]^k, \qquad \mathcal{H}_\lambda(z) = \frac{1 - z\, z_{J/\psi}}{z - z_{J/\psi}} \frac{1 - z\, z_{\psi(2S)}}{z - z_{\psi(2S)}} \phi_\lambda^{-1}(z) \sum_{k=0}^{2\,(4)} a_{\lambda,k} z^k$$

- Charm loop cannot fully explain SM discrepancies.
- Tension in C_9 is level of **1.9σ (1.8σ)** for without (with) LCSR results.

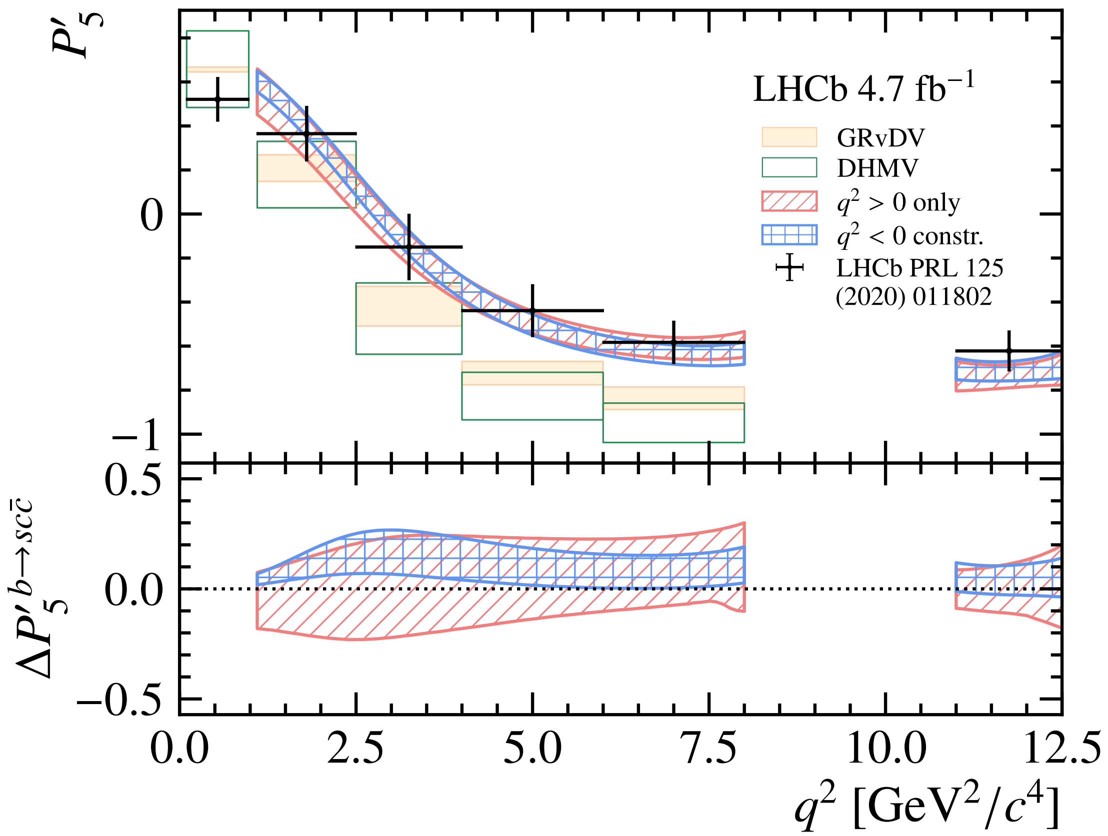

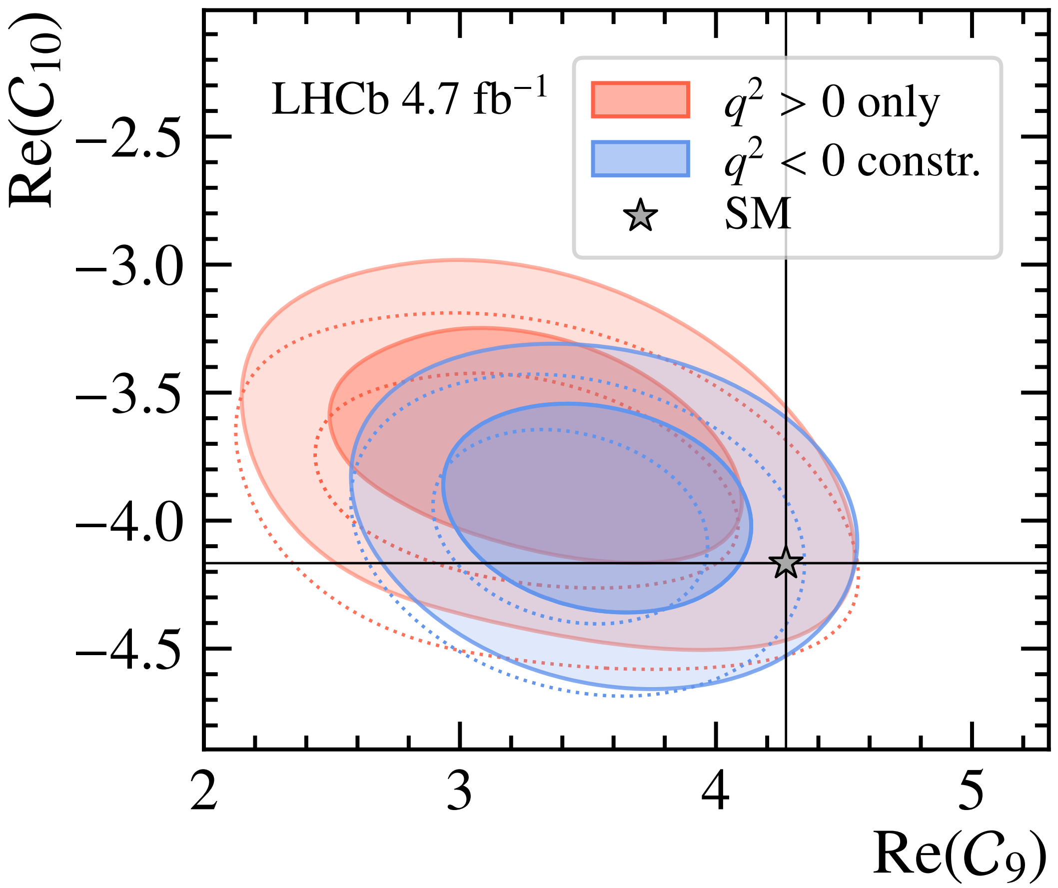

$$\Delta\mathcal{C}_9 = -0.93^{+0.53}_{-0.57} \quad (-0.68^{+0.33}_{-0.46})$$
$$\Delta\mathcal{C}_{10} = 0.48^{+0.29}_{-0.31} \quad (0.24^{+0.27}_{-0.28})$$
$$\Delta\mathcal{C}_9' = 0.48^{+0.49}_{-0.55} \quad (0.26^{+0.40}_{-0.48})$$
$$\Delta\mathcal{C}_{10}' = 0.38^{+0.28}_{-0.25} \quad (0.27^{+0.25}_{-0.27})$$

LHCb, 2312.09102; 2312.09115

Dispersion relations

Lyon &Zwicky, 1406.0566
Blake et al., 1709.03921
Cornella et al., 2001.04470
Bordone et al., 2401.18007

- LD contribution from charmonium resonances are taken into account with a subtracted dispersion relation.

$$\mathcal{C}_9^{(\mathrm{eff}),\lambda} = \mathcal{C}_9 + Y_{q\bar{q},\lambda}(q^2),$$

$$Y_{q\bar{q},\lambda}(q^2) = Y_{q\bar{q},\lambda}(q_0^2) + \frac{(q^2-q_0^2)}{\pi}\int_{4m_\mu^2}^{\infty}\frac{\rho_{q\bar{q},\lambda}(s)}{(s-q_0^2)(s-q^2-i\epsilon)}\mathrm{d}s$$

spectral density for an intermediate hadronic state

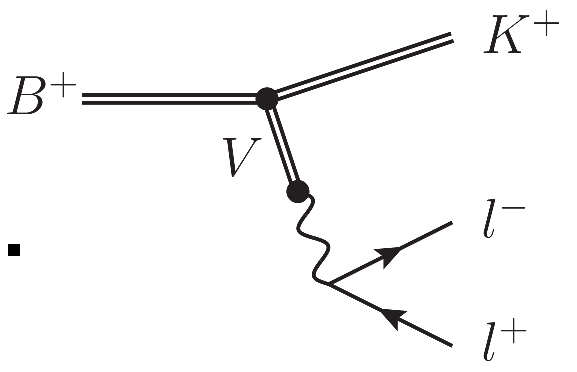

- Leading contribution is provided by single-particle states.

$$Y_{c\bar{c}}^{\lambda}(q^2) = -\frac{4}{9}\left[\frac{4}{3}C_1(\mu)+C_2(\mu)\right]\left[1+\ln\left(\frac{m^2}{\mu^2}\right)\right] + \frac{16\pi^2}{\mathcal{F}_\lambda(q^2)}\sum_V \eta_V^\lambda e^{i\delta_V^\lambda}\frac{q^2}{m_V^2}A_V^{\mathrm{res}}(q^2)$$

Breit-Wigner distribution: $A_V^{\mathrm{res}}(q^2) = \dfrac{m_V\Gamma_V}{m_V^2 - q^2 - i m_V\Gamma_V}$ *model uncertainty?*

- $\{\eta_V^\lambda,\ \delta_V^\lambda\}$ are determined from data on $B\to K^{(*)}V(\to\mu^+\mu^-)$.

Dispersion relations (cont'd)

Bordone et al., 2401.18007

- ✦ Fit results exhibit no significant q^2 and process dependences, *i.e.*, δC_9 is consistent with a SD NP effect, though uncertainties are still large.

$$B \to K \mu^+\mu^-$$

$V = J/\psi,\ \psi(2S),\ \psi(3770),\ \psi(4040),\ \psi(4160),\ \psi(4415)$

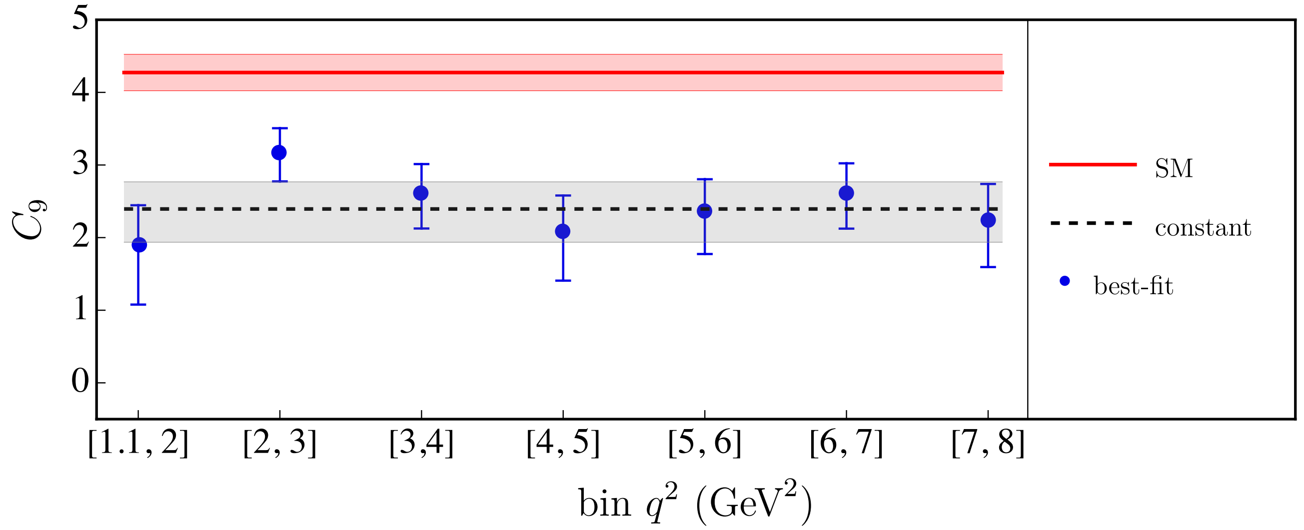

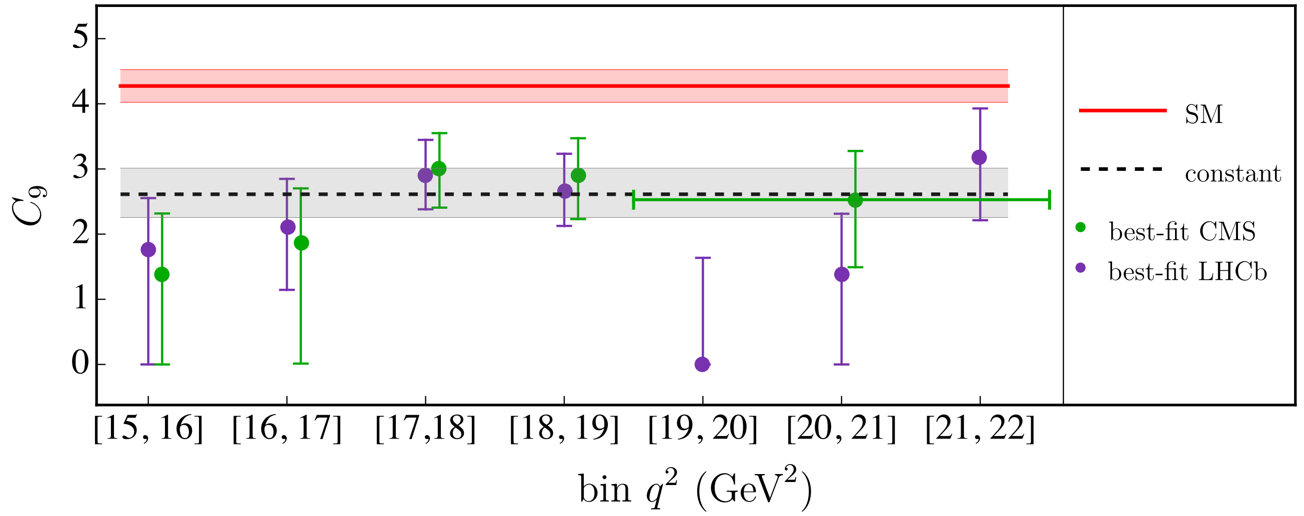

$$B \to K^*\mu^+\mu^-$$

$V = J/\psi,\ \psi(2S)$

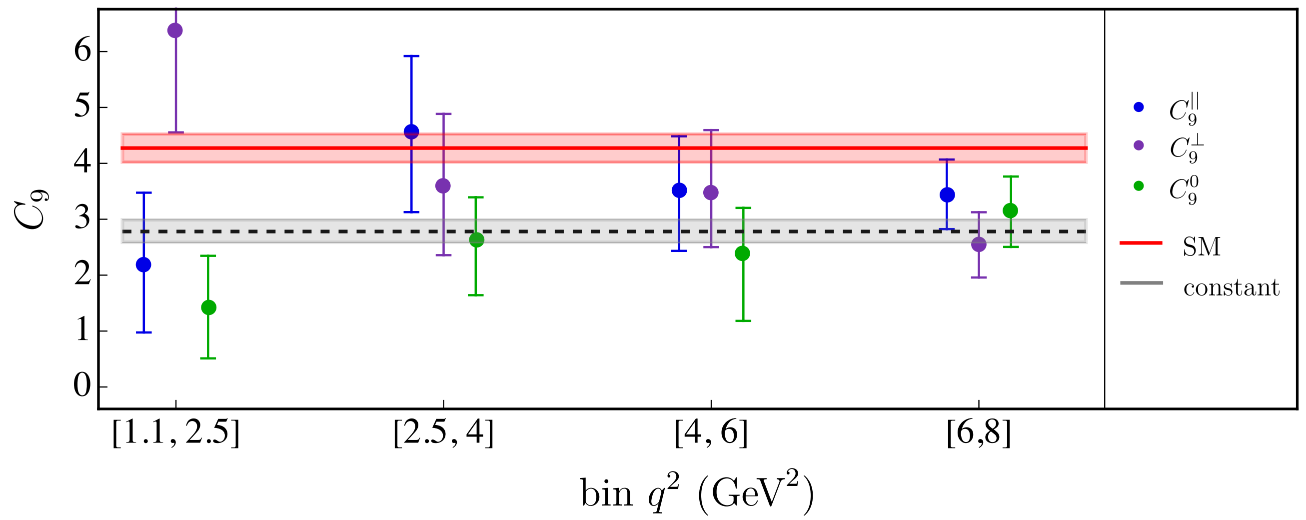

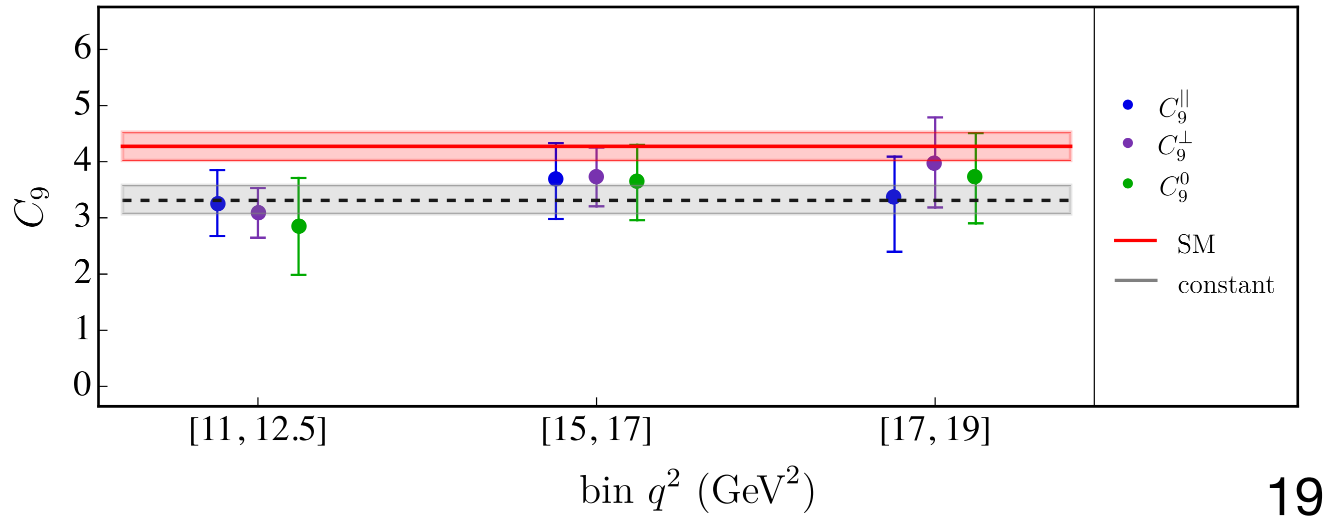

Dispersion relations (LHCb)

LHCb, 2405.17347

- Recently, LHCb has performed a comprehensive study including q^2 regions around charmonium resonances.

- In addition to one-particle states, two-particle states are taken into account.

$$\rho_{q\bar{q},\lambda}(q^2) = \rho^{\rm 1P}_{q\bar{q},\lambda}(q^2) + \rho^{\rm 2P}_{q\bar{q},\lambda}(q^2), \qquad j = \{\rho(770), \omega(782), \phi(1020), J/\psi, \psi(2S), \psi(3770), \psi(4040), \psi(4160)\}$$

$$\rho^{2P}_{q\bar{q}}(q^2) = \sum_k \left[\frac{\lambda(q^2, m^2_{k_1}, m^2_{k_2})}{q^2}\right]^{\frac{2L+1}{2}}$$

$k = \{D\overline{D}, D^*\overline{D}, D^*\overline{D}^*\}$

$L = 0$ for $D^*\overline{D}$, and $L = 1$ for $D\overline{D}$ and $D^*\overline{D}^*$ (lowest partial waves)

two-body phase-space function

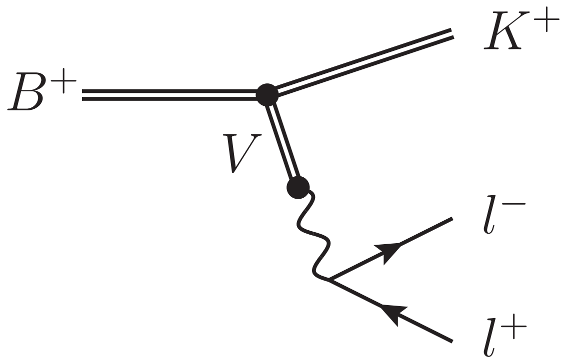

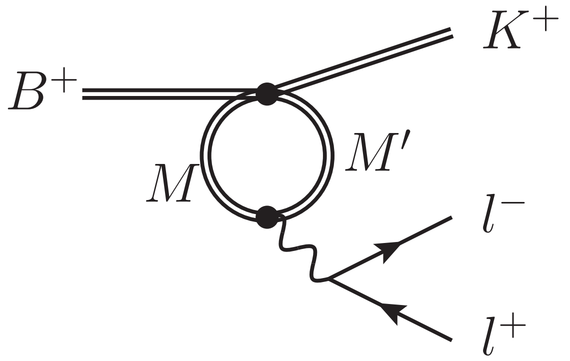

Cornella et al., 2001.04470
Bordone et al., 2401.18007

Dispersion relations (LHCb)

LHCb, 2405.17347

✦ Non-local amplitudes are determined from data.

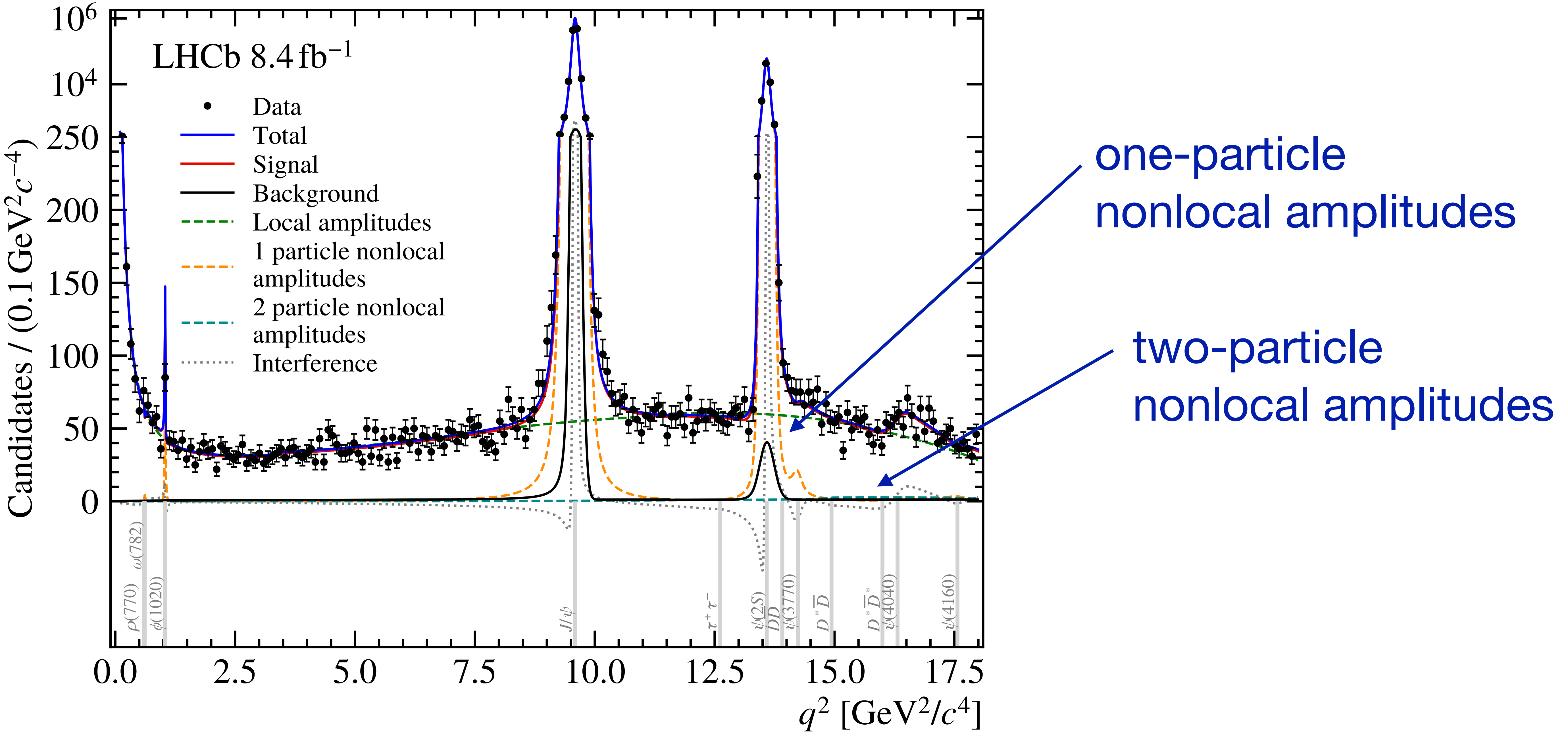

Dispersion relations (LHCb)

LHCb, 2405.17347

- Fit result for C_9 exhibits **2.1σ deviation** from SM.

Wilson Coefficient results	
$\mathcal{C}_9$	$3.56 \pm 0.28 \pm 0.18$
$\mathcal{C}_{10}$	$-4.02 \pm 0.18 \pm 0.16$
$\mathcal{C}_9'$	$0.28 \pm 0.41 \pm 0.12$
$\mathcal{C}_{10}'$	$-0.09 \pm 0.21 \pm 0.06$
$\mathcal{C}_{9\tau}$	$(-1.0 \pm 2.6 \pm 1.0) \times 10^2$

$$\Delta\mathcal{C}_9^{\rm NP} = -0.71 \pm 0.33$$

$|\mathcal{C}_{9\tau}| < 500$ @ 90% CL

similar to Belle limit on $\mathcal{B}(B^0 \to K^{*0}\tau^+\tau^-)$

- Data prefers larger nonlocal contributions than LCSR estimate.

- Although nonlocal contributions play a clear role in P_5', tension in C_9 persists.

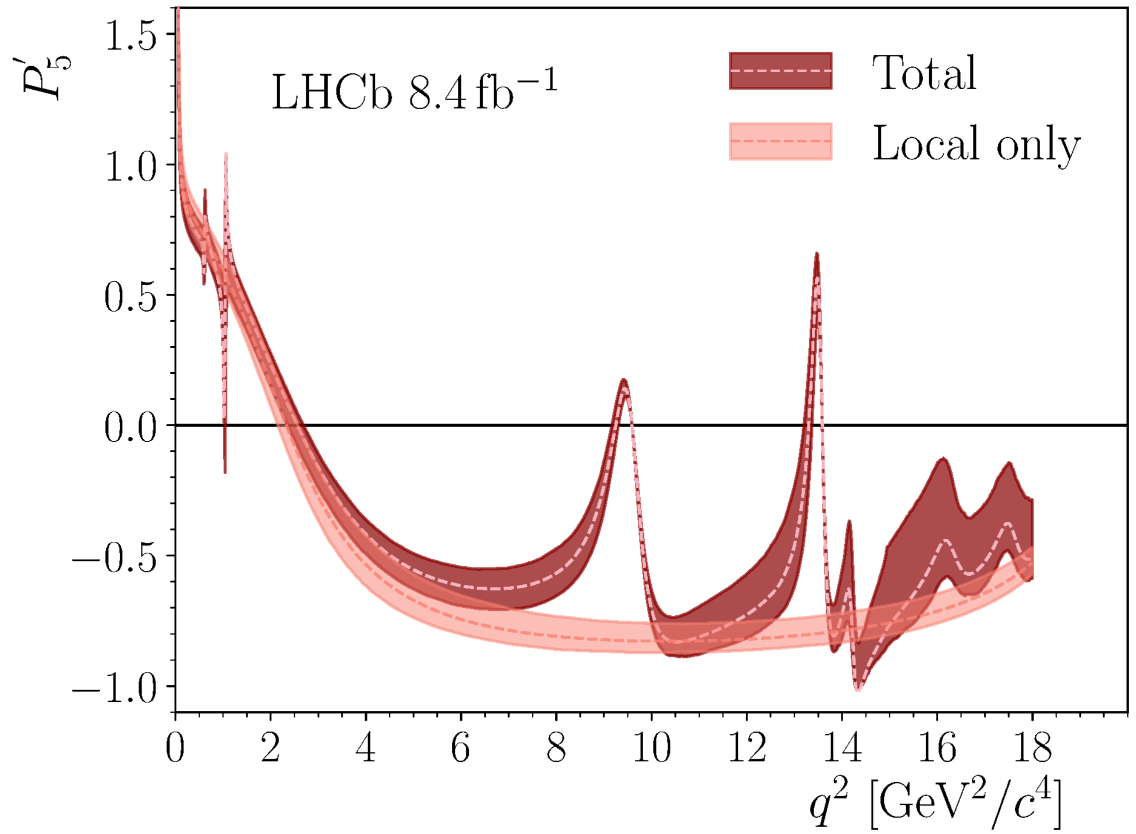

LHCb results

- Two LHCb results obtained with different models are compatible with each other.

z-expansion with analyticity

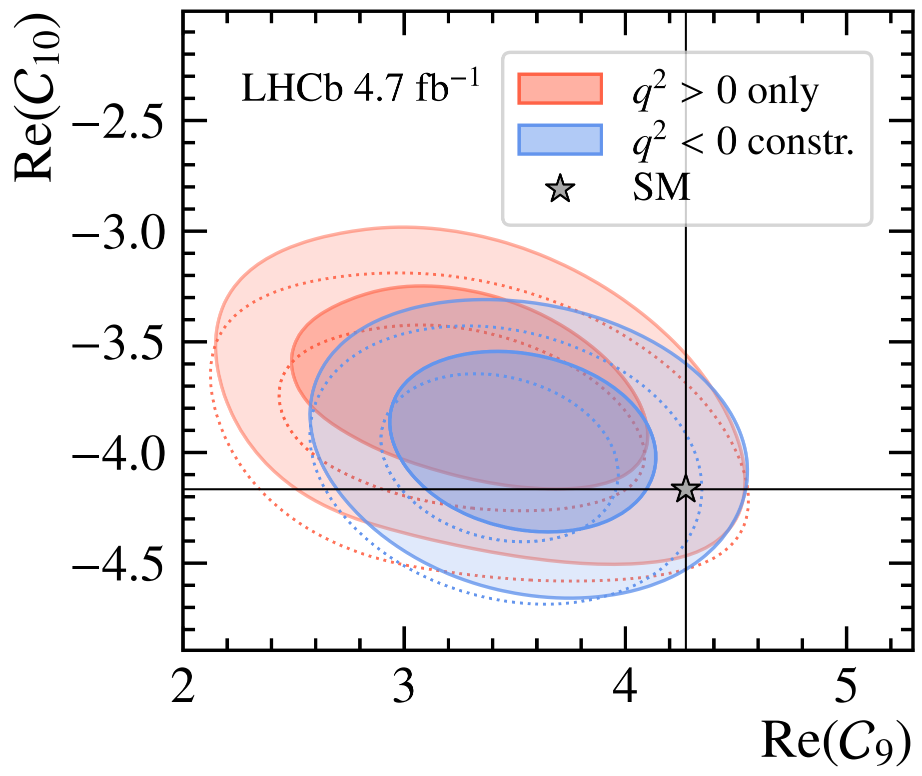

dispersion relations
1σ, 3σ; stat. only and stat.+syst.

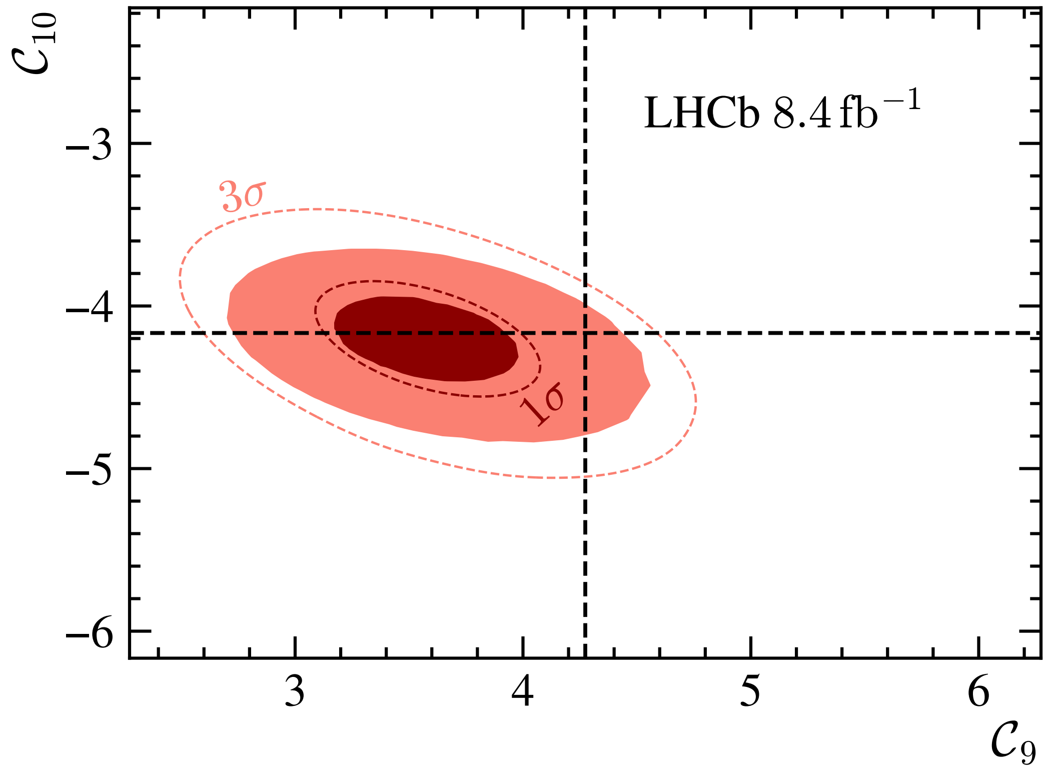

discrepancy in imaginary part of LD contribution

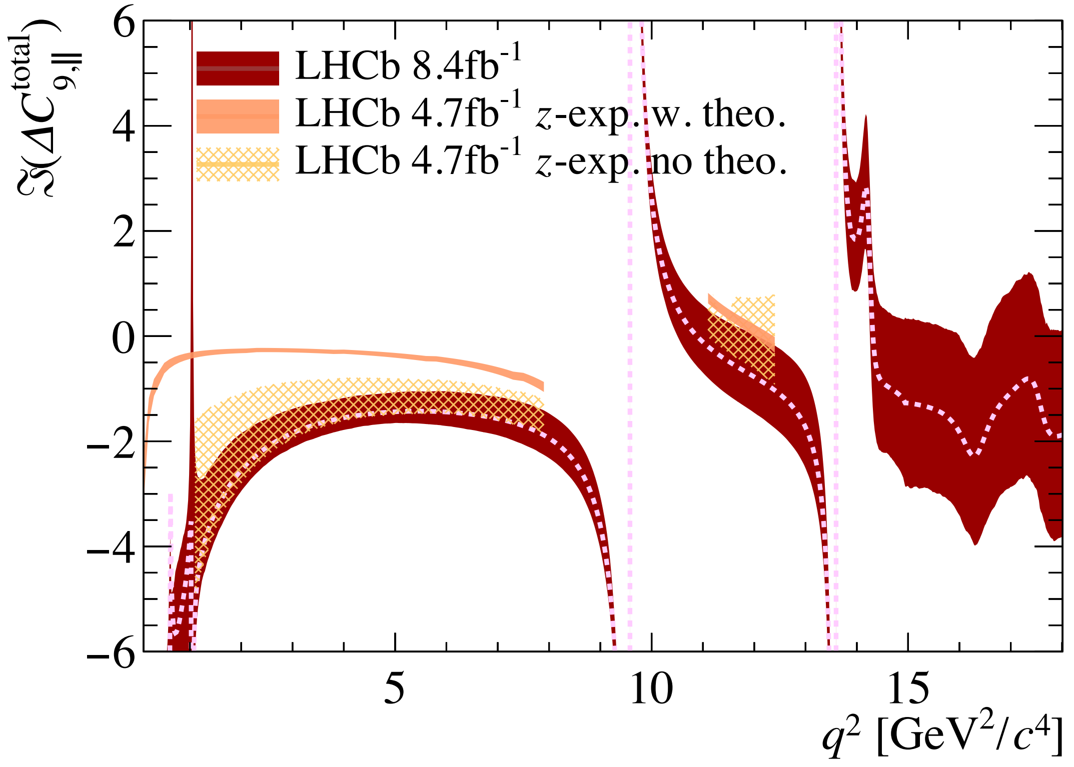

model dependence?

Charm rescattering

- Charm rescattering has been estimated using *Isidori et al., 2405.17551*
  - an effective description in terms of hadronic degrees of freedom,
  - a vector-meson-dominance ansatz for EM form factor, and
  - heavy-hadron chiral perturbation theory.

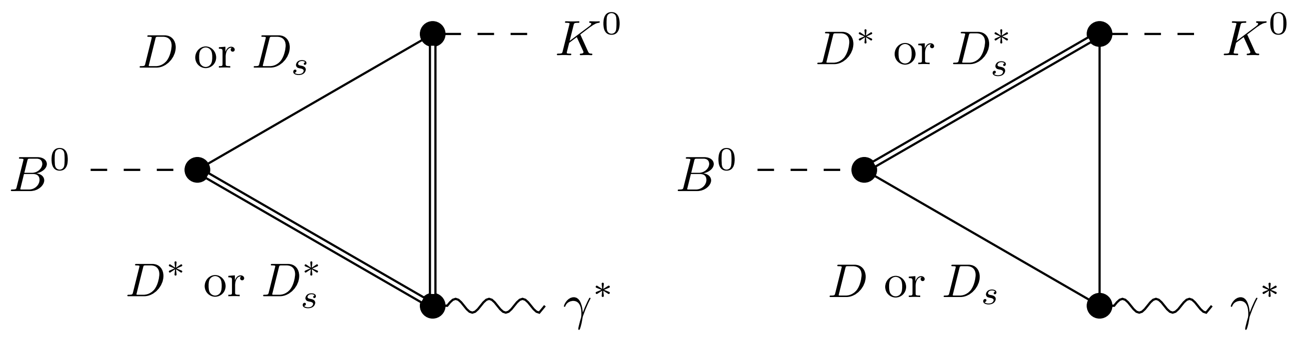

- LD amplitude does not exceed a few percent relative to SD one.
- At most 10% shift in C_9.

$$|\delta C_9^{\mathrm{LD}}| \leq \mathcal{N} |\delta \bar{C}_{9,DD^*}^{\mathrm{LD}}| \leq 0.33$$

$$\mathcal{N} = \frac{\sum_X \mathcal{B}(B^0 \to X)}{\mathcal{B}(B^0 \to D^* D_s) + \mathcal{B}(B^0 \to D D_s^*)} \approx 3$$

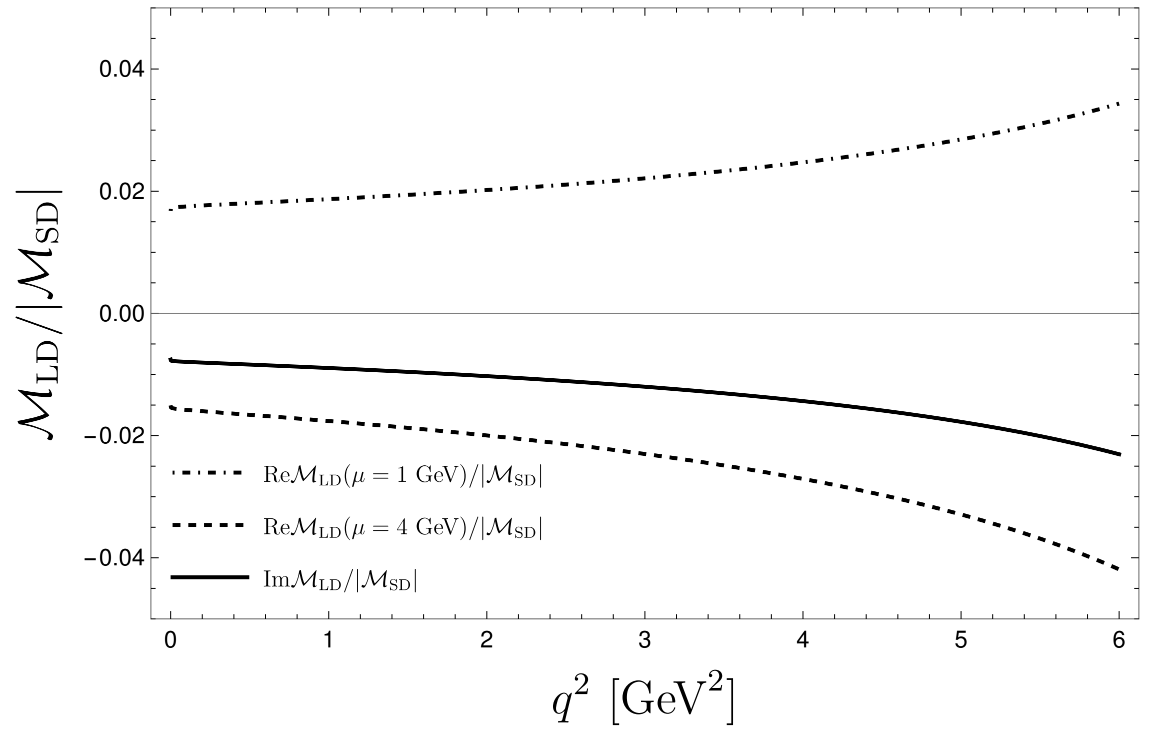

Global fit and NP interpretation

SM predictions

Alguero et al., 2304.07330

- ✦ LD contributions in low q^2 are evaluated using LCSR result.
- ✦ Tensions in several observables.

$10^7 \times B(B^+ \to K^+\mu\mu)$ [LHCb]	SM	Experiment [3]	Pull
$[0.1, 0.98]$	0.32 ± 0.03	0.29 ± 0.02	$+0.9$
$[1.1, 2.]$	0.33 ± 0.03	0.21 ± 0.02	$+4.0$
$[2., 3.]$	0.37 ± 0.03	0.28 ± 0.02	$+2.5$
$[3., 4.]$	0.37 ± 0.03	0.25 ± 0.02	$+3.4$
$[4., 5.]$	0.37 ± 0.03	0.22 ± 0.02	$+4.4$
$[5., 6.]$	0.37 ± 0.03	0.23 ± 0.02	$+4.0$
$[6., 7.]$	0.37 ± 0.03	0.25 ± 0.02	$+3.3$
$[7., 8.]$	0.38 ± 0.04	0.23 ± 0.02	$+3.1$
$[15., 22.]$	1.15 ± 0.16	0.85 ± 0.05	$+1.8$
$10^7 \times B(B^0 \to K^0\mu\mu)$ [LHCb]	SM	Experiment [3]	Pull
$[0.1, 2.]$	0.65 ± 0.05	0.23 ± 0.11	$+3.4$
$[2., 4.]$	0.69 ± 0.05	0.37 ± 0.11	$+2.5$
$[4., 6.]$	0.69 ± 0.05	0.35 ± 0.11	$+2.8$
$[6., 8.]$	0.69 ± 0.07	0.54 ± 0.12	$+1.1$
$[15., 22.]$	1.07 ± 0.15	0.67 ± 0.12	$+2.1$

$10^7 \times B(B^0 \to K^{*0}\mu\mu)$ [LHCb]	SM	Experiment [4]	Pull
$[0.1, 0.98]$	0.76 ± 0.45	0.89 ± 0.09	-0.3
$[1.1, 2.5]$	0.50 ± 0.25	0.46 ± 0.06	$+0.2$
$[2.5, 4.]$	0.53 ± 0.26	0.50 ± 0.06	$+0.1$
$[4., 6.]$	0.81 ± 0.44	0.71 ± 0.07	$+0.2$
$[6., 8.]$	0.97 ± 0.62	0.86 ± 0.08	$+0.2$
$[15., 19.]$	2.54 ± 0.23	1.74 ± 0.14	$+3.0$
$10^7 \times B(B^+ \to K^{*+}\mu\mu)$ [LHCb]	SM	Experiment [3]	Pull
$[0.1, 2.]$	1.19 ± 0.67	1.12 ± 0.27	$+0.1$
$[2., 4.]$	0.76 ± 0.37	1.12 ± 0.32	-0.7
$[4., 6.]$	0.88 ± 0.48	0.50 ± 0.20	$+0.7$
$[6., 8.]$	1.06 ± 0.67	0.66 ± 0.22	$+0.6$
$[15., 19.]$	2.74 ± 0.25	1.60 ± 0.32	$+2.8$
$10^7 \times B(B_s \to \phi\mu\mu)$ [LHCb]	SM	Experiment [5]	Pull
$[0.1, 0.98]$	1.10 ± 0.56	0.68 ± 0.06	$+0.7$
$[1.1, 2.5]$	0.71 ± 0.32	0.44 ± 0.05	$+0.9$
$[2.5, 4.]$	0.74 ± 0.37	0.35 ± 0.04	$+1.0$
$[4., 6.]$	1.11 ± 0.70	0.62 ± 0.06	$+0.7$
$[6., 8.]$	1.32 ± 1.09	0.63 ± 0.06	$+0.6$
$[15., 19.]$	2.34 ± 0.15	1.81 ± 0.12	$+2.7$
$P_5'(B^0 \to K^{*0}\mu\mu)$ [LHCb]	SM	Experiment [6]	Pull
$[0.1, 0.98]$	0.68 ± 0.14	0.52 ± 0.10	$+0.9$
$[1.1, 2.5]$	0.20 ± 0.13	0.37 ± 0.12	-0.9
$[2.5, 4.]$	-0.43 ± 0.12	-0.15 ± 0.15	-1.5
$[4., 6.]$	-0.72 ± 0.08	-0.44 ± 0.12	-1.9
$[6., 8.]$	-0.81 ± 0.08	-0.58 ± 0.09	-1.9
$[15., 19.]$	-0.57 ± 0.05	-0.67 ± 0.06	$+1.2$

Global fit

- 2D fit of $C_{9\mu}$ and $C_{10\mu}$ prefers a negative shift of O(20%) in $C_{9\mu}$.
  - Preferred values for $C_{9\mu}$ are consistent throughout different observables.

Alguero et al., 2304.07330

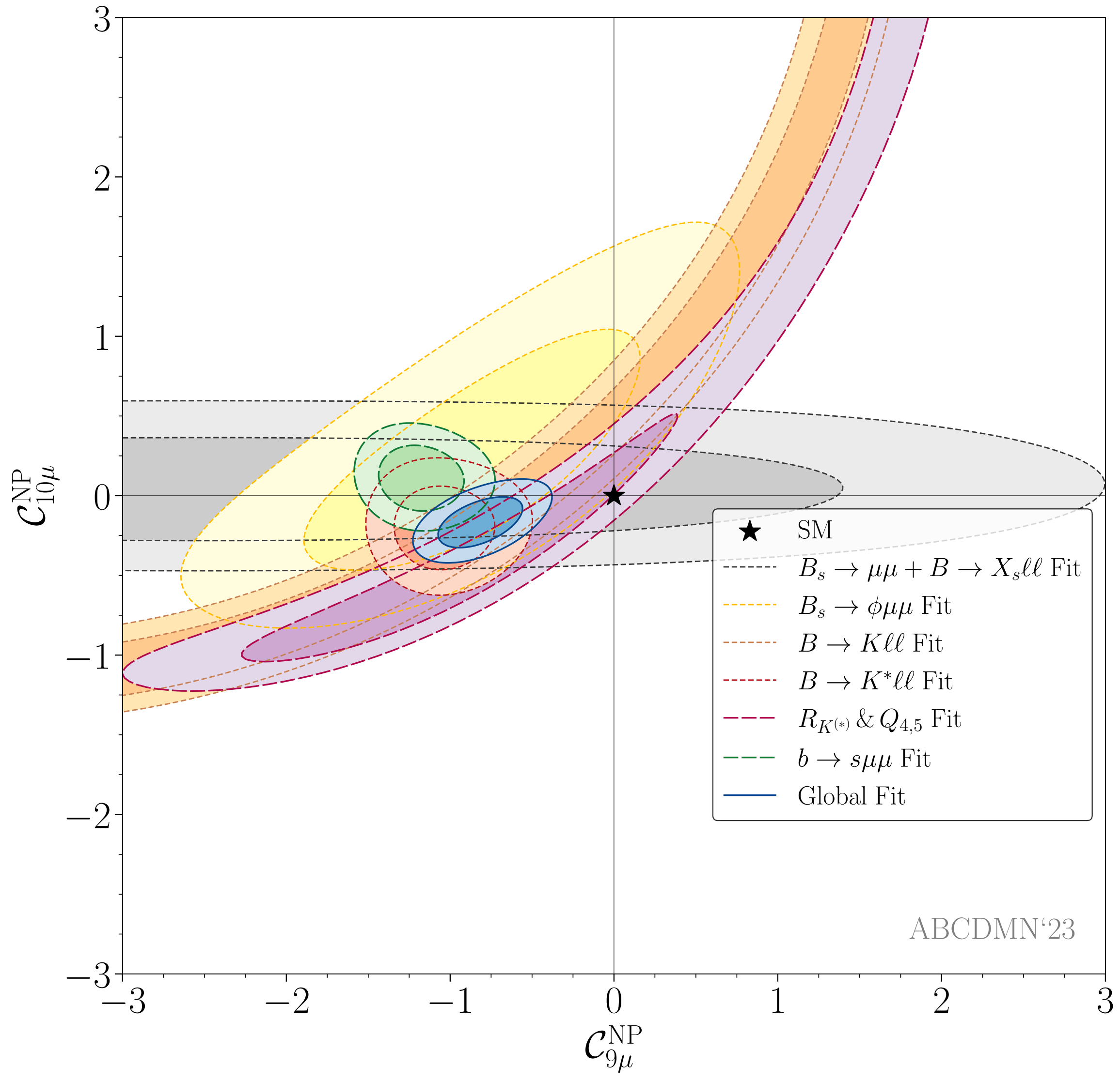

- Consistent with other groups.

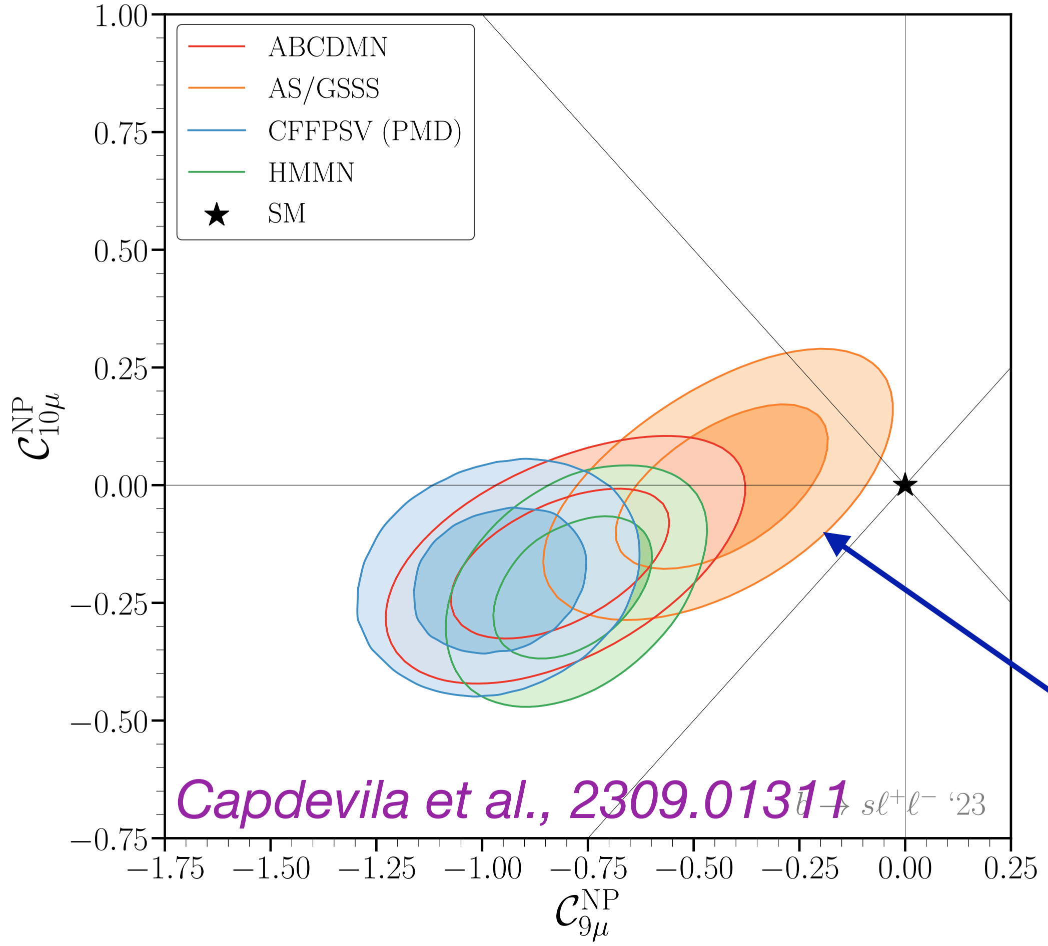

Alguero et al., 2304.07330
Greljo et al. [flavio], 2212.10497
Ciuchini et al. [HEPfit], 2212.10516
Hurth et al.[SuperIso], 2310.05585

no $q^2 > 6$ GeV^2 data

Data-driven fit

✦ Current data are consistent with SM in a ***data-driven*** approach.

$$
\begin{aligned}
h_-(q^2) &= -\frac{m_b}{8\pi^2 m_B}\widetilde{T}_{L-}(q^2)h_-^{(0)} - \frac{\widetilde{V}_{L-}(q^2)}{16\pi^2 m_B^2}h_-^{(1)}q^2 \\
&\quad + h_-^{(2)}q^4 + \mathcal{O}(q^6)\,, \\
h_+(q^2) &= -\frac{m_b}{8\pi^2 m_B}\widetilde{T}_{L+}(q^2)h_-^{(0)} - \frac{\widetilde{V}_{L+}(q^2)}{16\pi^2 m_B^2}h_-^{(1)}q^2 \\
&\quad + h_+^{(0)} + h_+^{(1)}q^2 + h_+^{(2)}q^4 + \mathcal{O}(q^6)\,, \\
h_0(q^2) &= -\frac{m_b}{8\pi^2 m_B}\widetilde{T}_{L0}(q^2)h_-^{(0)} - \frac{\widetilde{V}_{L0}(q^2)}{16\pi^2 m_B^2}h_-^{(1)}q^2 \\
&\quad + h_0^{(0)}\sqrt{q^2} + h_0^{(1)}(q^2)^{\frac{3}{2}} + \mathcal{O}((q^2)^{\frac{5}{2}})\,. \qquad (11)
\end{aligned}
$$

Ciuchini et al., 2212.10516

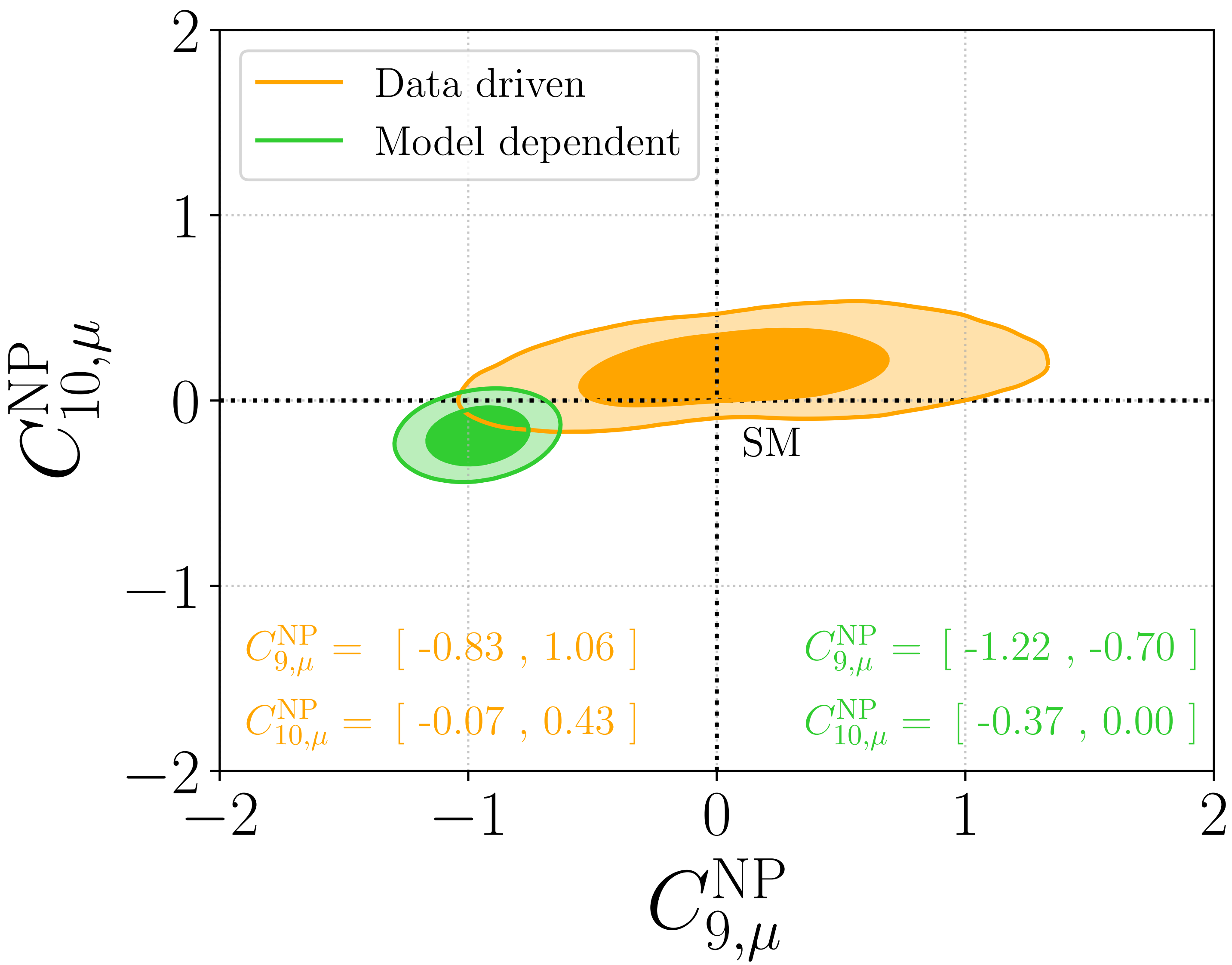

LFU or LFUV

- Since $R_{K^{(*)}}$ data strongly constrain LFUV NP, dominant NP contributions need to be LFU.

$$\mathcal{C}_{i\,e} = \mathcal{C}_i^{\mathrm{U}}\,, \qquad \mathcal{C}_{i\,\mu} = \mathcal{C}_i^{\mathrm{U}} + \mathcal{C}_{i\,\mu}^{\mathrm{V}}$$

- Preferred scenarios: *Alguero et al., 2304.07330*

Scenario	Best-fit point	1σ	$\mathrm{Pull}_{\mathrm{SM}}$	p-value
$\mathcal{C}_{9\mu}^{\mathrm{NP}} = \mathcal{C}_{9e}^{\mathrm{NP}} = \mathcal{C}_9^{\mathrm{U}}$	-1.17	$[-1.33, -1.00]$	5.8	39.9 %
$\mathcal{C}_{9\mu}^{\mathrm{V}}$	-0.21	$[-0.39, -0.02]$	5.6	40.3 %
$\mathcal{C}_9^{\mathrm{U}}$	-0.97	$[-1.21, -0.72]$		
$\mathcal{C}_{9\mu}^{\mathrm{V}} = -\mathcal{C}_{10\mu}^{\mathrm{V}}$	-0.08	$[-0.14, -0.02]$	5.6	41.1 %
$\mathcal{C}_9^{\mathrm{U}}$	-1.10	$[-1.27, -0.91]$		

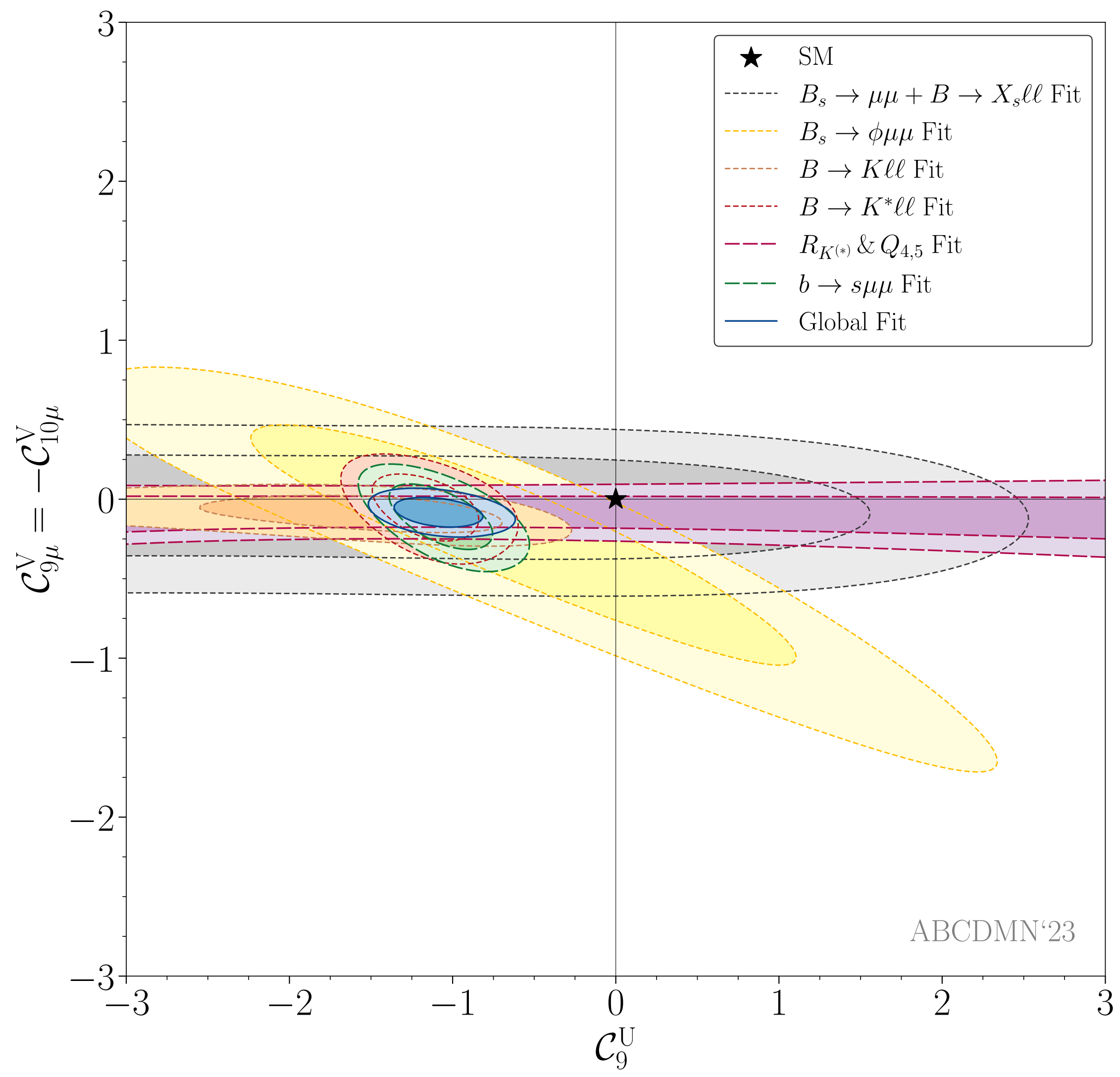

- $Q_5 = P'_{5\mu} - P'_{5e}$ should be measured close to zero.

- 3rd scenario has a model-independent connection to $R(D^{(*)})$.

Test for charm loop

- ✦ No significant evidence for non-constant q^2 and process dependencies.

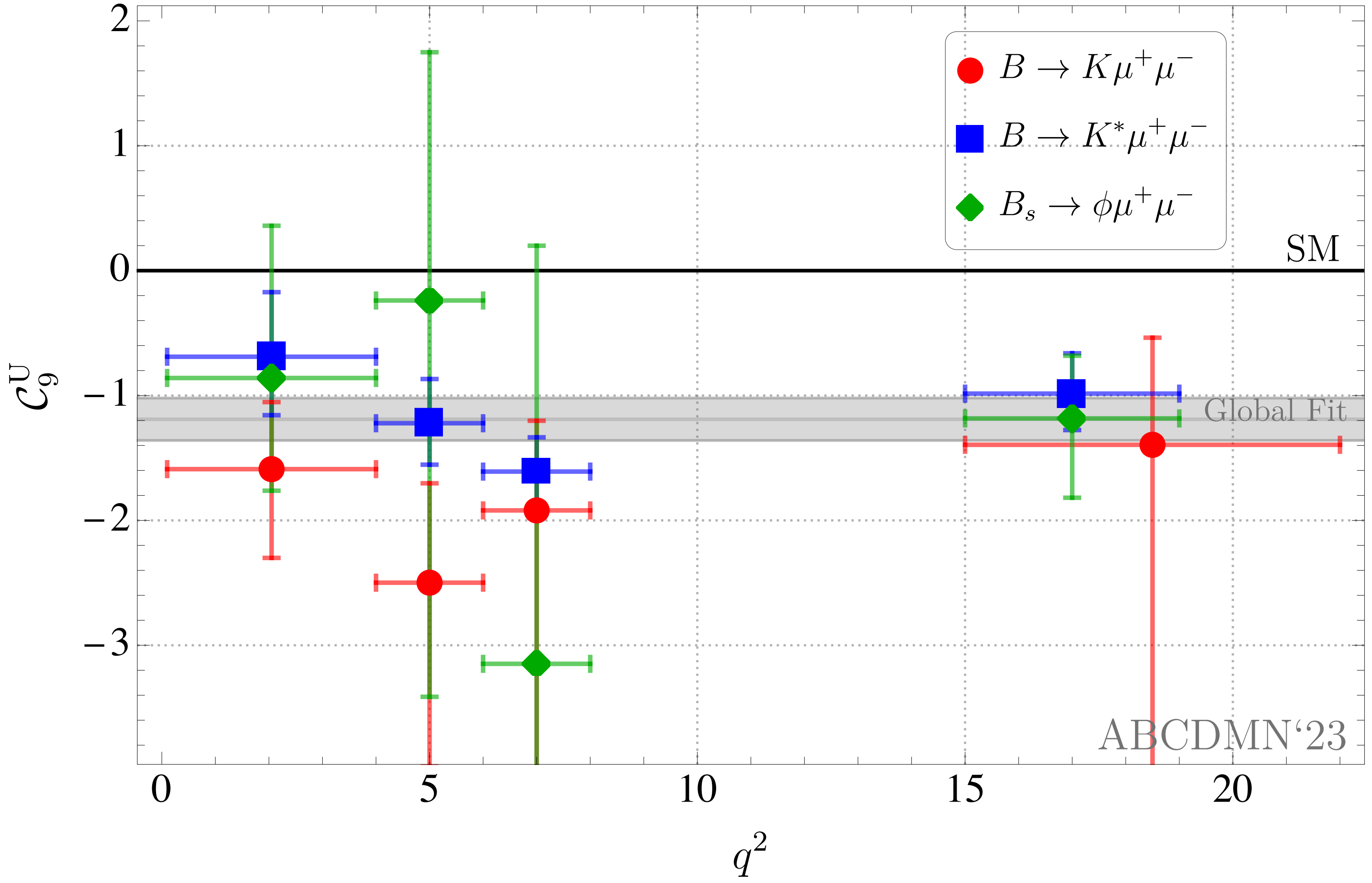

Alguero et al., 2304.07330

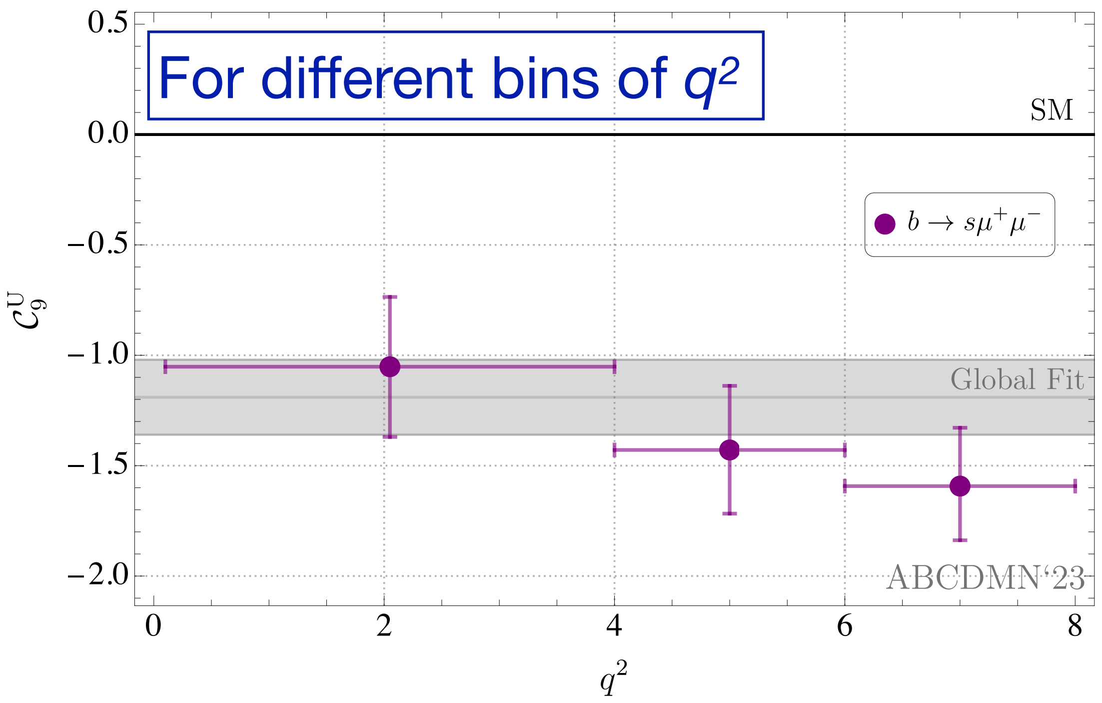

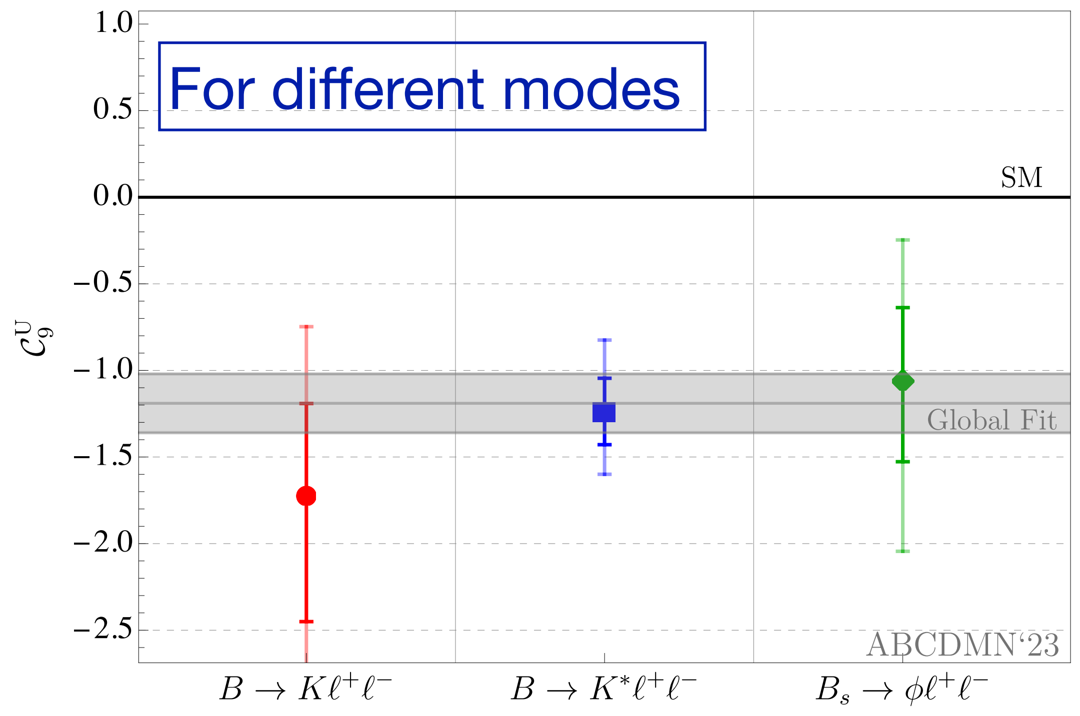

SMEFT at tree

- SMEFT operators: $\mathcal{O}^{(1)}_{ijkl} = (\bar{Q}_i \gamma^\mu Q_j)(\bar{L}_k \gamma_\mu L_l)$, $\quad \mathcal{O}^{(3)}_{ijkl} = (\bar{Q}_i \gamma^\mu \sigma^a Q_j)(\bar{L}_k \gamma_\mu \sigma^a L_l)$

$$C^{(1)}_{23ij}\mathcal{O}^{(1)}_{23ij} + C^{(3)}_{23ij}\mathcal{O}^{(3)}_{23ij} = 2C^{(3)}_{23ij}\left[V_{cs}\underline{(\bar{c}_L\gamma^\mu b_L)(\bar{\ell}_{Li}\gamma_\mu \nu_{Lj})} + V^*_{tb}(\bar{s}_L\gamma^\mu t_L)(\bar{\nu}_{Li}\gamma_\mu \ell_{Lj})\right] \quad \boldsymbol{b \to c\tau\bar{\nu}}$$

$$+\left(C^{(1)}_{23ij} + C^{(3)}_{23ij}\right)\left[\underline{(\bar{s}_L\gamma^\mu b_L)(\bar{\ell}_{Li}\gamma_\mu \ell_{Lj})} + V^*_{tb}V_{cs}(\bar{c}_L\gamma^\mu t_L)(\bar{\nu}_{Li}\gamma_\mu \nu_{Lj})\right] \quad \begin{array}{l}\boldsymbol{b \to s\mu\bar{\mu}}\\ \boldsymbol{b \to s\tau\bar{\tau}}\end{array}$$

$$+\left(C^{(1)}_{23ij} - C^{(3)}_{23ij}\right)\left[\underline{(\bar{s}_L\gamma^\mu b_L)(\bar{\nu}_{Li}\gamma_\mu \nu_{Lj})} + V^*_{tb}V_{cs}(\bar{c}_L\gamma^\mu t_L)(\bar{\ell}_{Li}\gamma_\mu \ell_{Lj})\right] \quad \boldsymbol{b \to s\nu\bar{\nu}}$$

- $C^{(1)}_{23ij} = C^{(3)}_{23ij}$ for $\mathcal{B}(B \to K^{(*)}\nu\bar{\nu})$

- $|C^{(1,3)}_{2333}| \gg |C^{(1,3)}_{2311}| \sim |C^{(1,3)}_{2322}|$ for *B* anomalies

- Br's for $b \to s\tau\bar{\tau}$ are about two orders of magnitude larger than SM values.

$$C^{\rm NP}_{9,\tau} = -C^{\rm NP}_{10,\tau} \approx -\frac{2\pi}{\alpha}\frac{V_{cb}}{V_{tb}V^*_{ts}}\left(\sqrt{R_{D^{(*)}}/R^{\rm SM}_{D^{(*)}}} - 1\right)$$

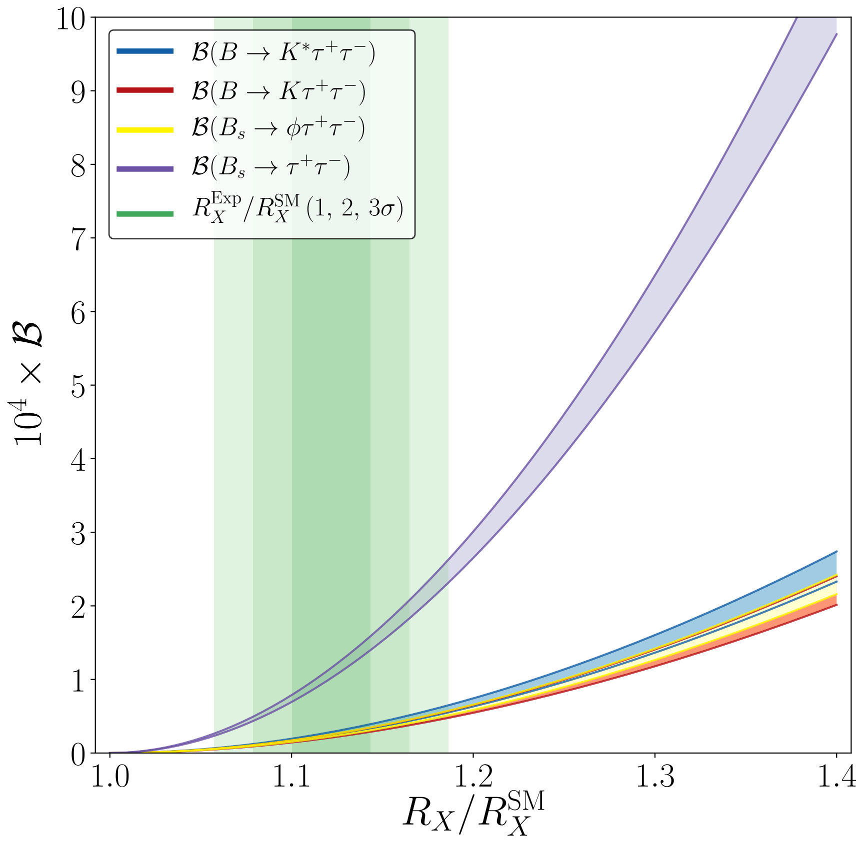

Capdevila et al., 1712.01919; Capdevila, PoS FPCP2023

SMEFT at one loop

- $\mathcal{O}_{2333}^{(1,3)}$ explains *R(D^(*))*, and generates C_9^{U} through one-loop mixing.

$$C_9^{\mathrm{U}} \approx 7.5\left(\sqrt{1 - R_{D^{(*)}}/R_{D^{(*)}}^{\mathrm{SM}}}\right)\left(1 + \frac{\log(\Lambda^2/(1\,\mathrm{TeV}^2))}{10.5}\right)$$

  - C_9^{U} arises from tau loop.
  - $C_{9,\mu}^{\mathrm{V}} = -C_{10,\mu}^{\mathrm{V}}$ arises at tree level.

- *$R(D^{(*)})$* imply $C_9^{\mathrm{U}} \approx -0.6$ for $\Lambda = 2$ TeV.
- $C_9^{\mathrm{U}} \approx -1.1$ corresponds to higher NP scale, $\Lambda = O(100\,\mathrm{TeV})$, which is incompatible with *$R(D^{(*)})$*.

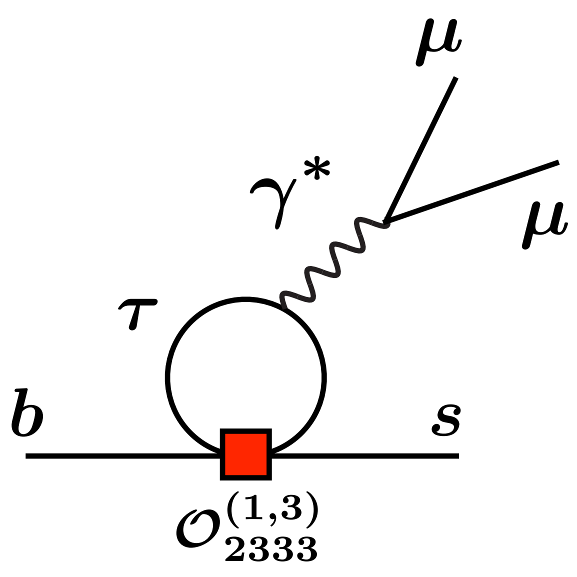

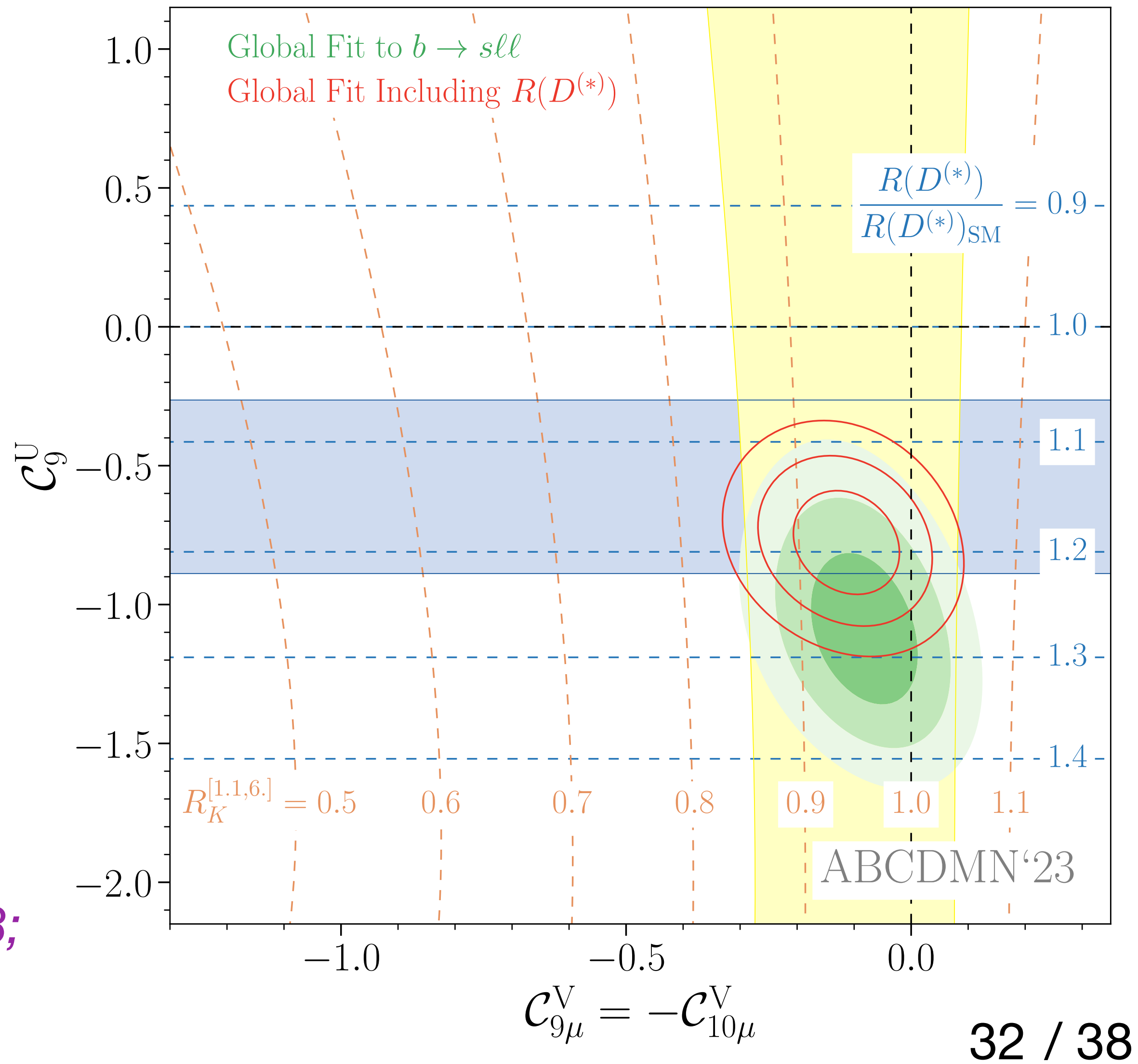

Alguero et al., 1903.09578; 2205.15212; 2304.07330

NP models

- $b \to s$ anomalies favor LFU NP in C_9^{U} with a size of 20% w.r.t. SM.
- *Z'* can have LFU couplings, but they receive severe constraints from *Bs* mixing, LHC limits, and $e^+e^- \to \ell^+\ell^-$ at LEP-II. *Greljo et al., 2212.10497*
- Leptoquark (LQ) with tree-level contributions require fine tuning. Moreover, to avoid LFV ($\mu \to e\gamma$), for instance, multiple LQ generations are introduced. *Crivellin et al., 2203.10111*
- One-loop contributions with tau or charm can generate C_9^{U}.

U_1, S_1+S_3, R_2 (S_2)

Crivellin et al., 1807.02068
Crivellin et al., 1912.04224
Crivellin et al., 2203.10111

H^+

Iguro & Omura, 1802.01732
Kumar, 2212.07233
Iguro, 2302.08935

LQ models

LQ Model	Wilson Coeff.	$b \to c$	$b \to s$	$b \to c + b \to s$
S_1	$C^{\text{BSM}}_{b_L\mu_L}, C^{\text{BSM}}_{b_L\mu_R}, C_{V_L}, C_{S_L} = -4C_T$	✓	✓	✓
R_2	$C^{\text{BSM}}_{b_L\mu_R}, C_{S_L} = 4C_T$	✓	✓	(✓)
S_3	$C^{\text{BSM}}_{b_L\mu_L}, C_{V_L}$	×	✓	×
U_1	$C^{\text{BSM}}_{b_L\mu_L}, C_{V_L}$	✓	✓	(✓)
V_2	$C^{\text{BSM}}_{b_L\mu_R}, C_{S_R}$	✓	✓	(✓)
U_3	$C^{\text{BSM}}_{b_L\mu_L}, C_{V_L}$	×	✓	×

Table 5: Summary of leptoquark models and the relevant BSM Wilson coefficients they predict at the effective level. Checkmarks denote models successfully explaining clean observables for a particular flavor transition, while crosses signify otherwise. The final column indicates whether the model can explain both sectors simultaneously. Models marked with (✓) reproduce experimental data with small muonic coefficients.

D' Alise et al., 2403.17614

$b \to s\, e\, e$

- LFU NP $C_9^{\mathrm{U}} = C_{9,e} \approx C_{9,\mu}$ would generate deviations from SM in *b*→*see* observables.

- New LHCb results at ICHEP2024 are consistent with SM and with LFU hypothesis.

Coutinho [LHCb], ICHEP2024

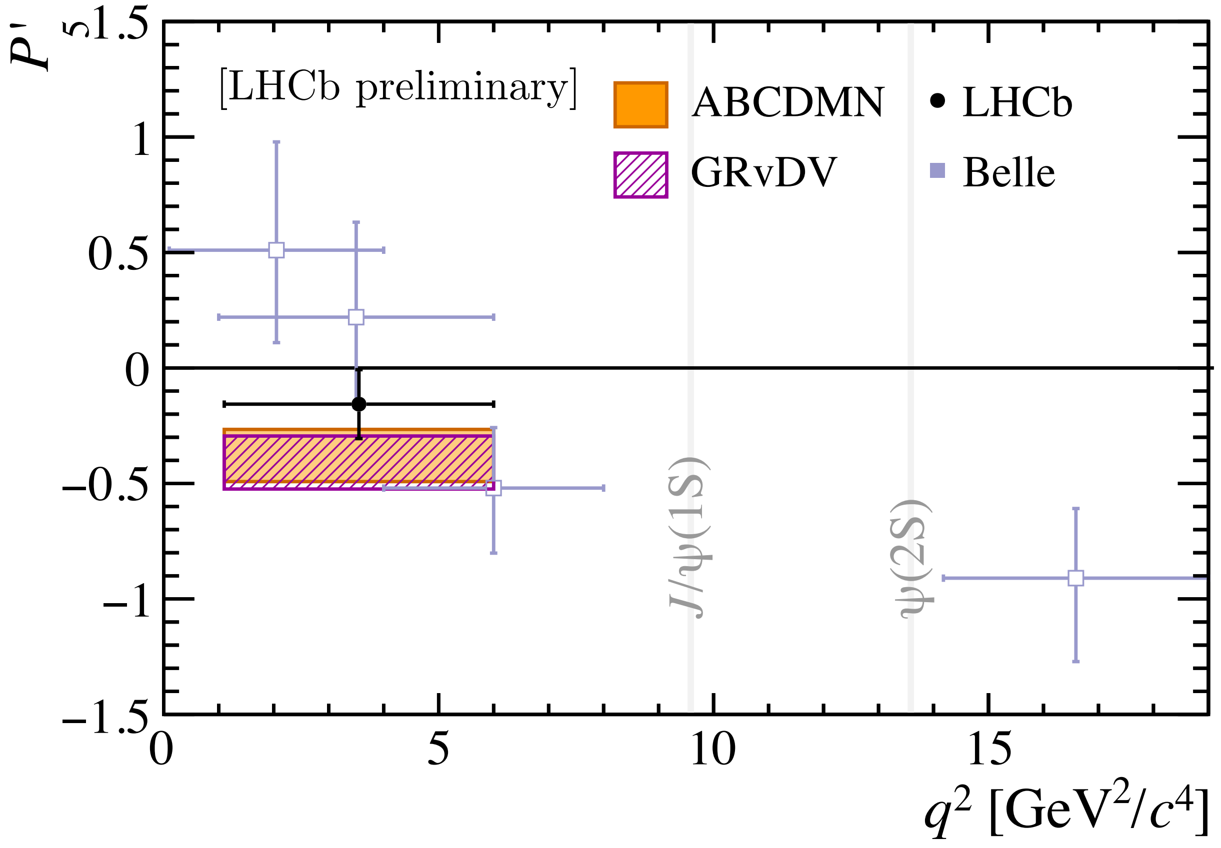

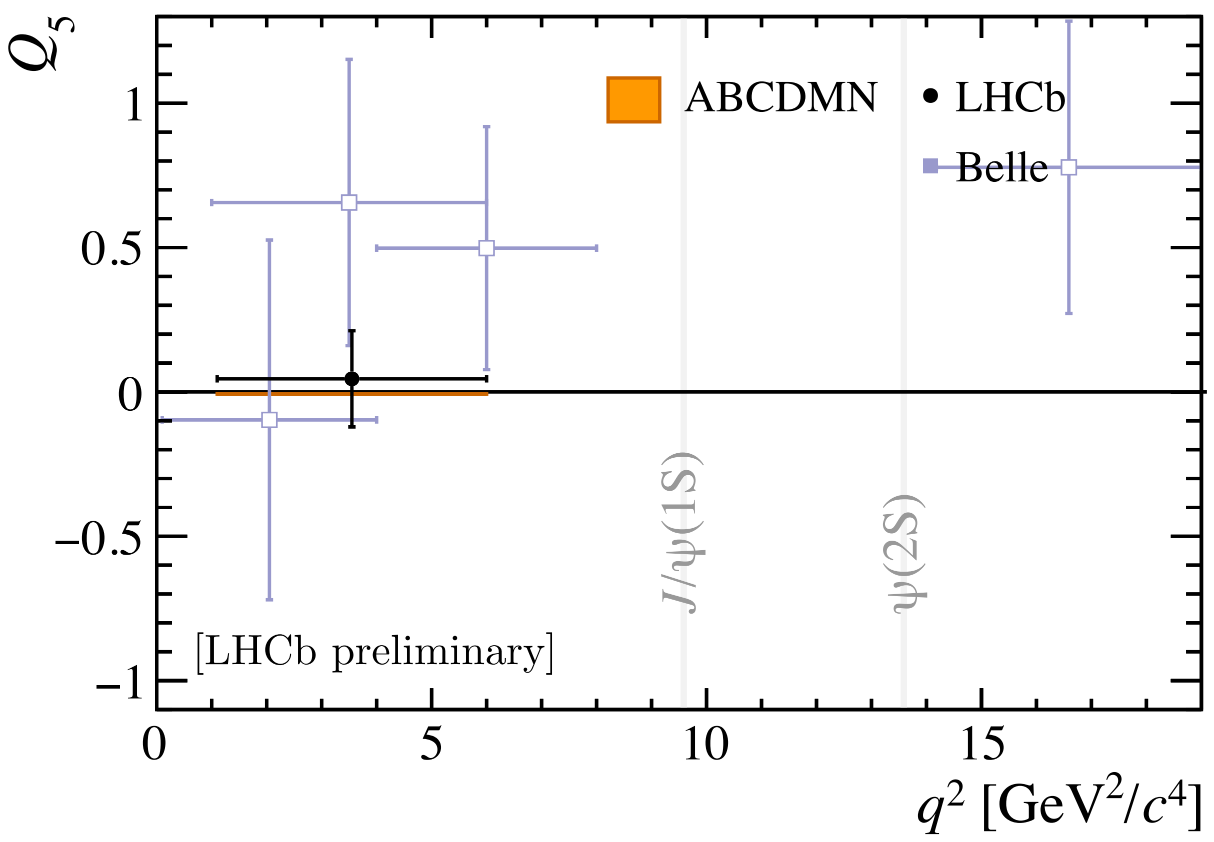

Inclusive measurement

- ✦ Inclusive measurement consistent with SM would exclude $C_9^{\rm NP} \approx -1$ at high confidence.

Huber et al., 2404.03517

current

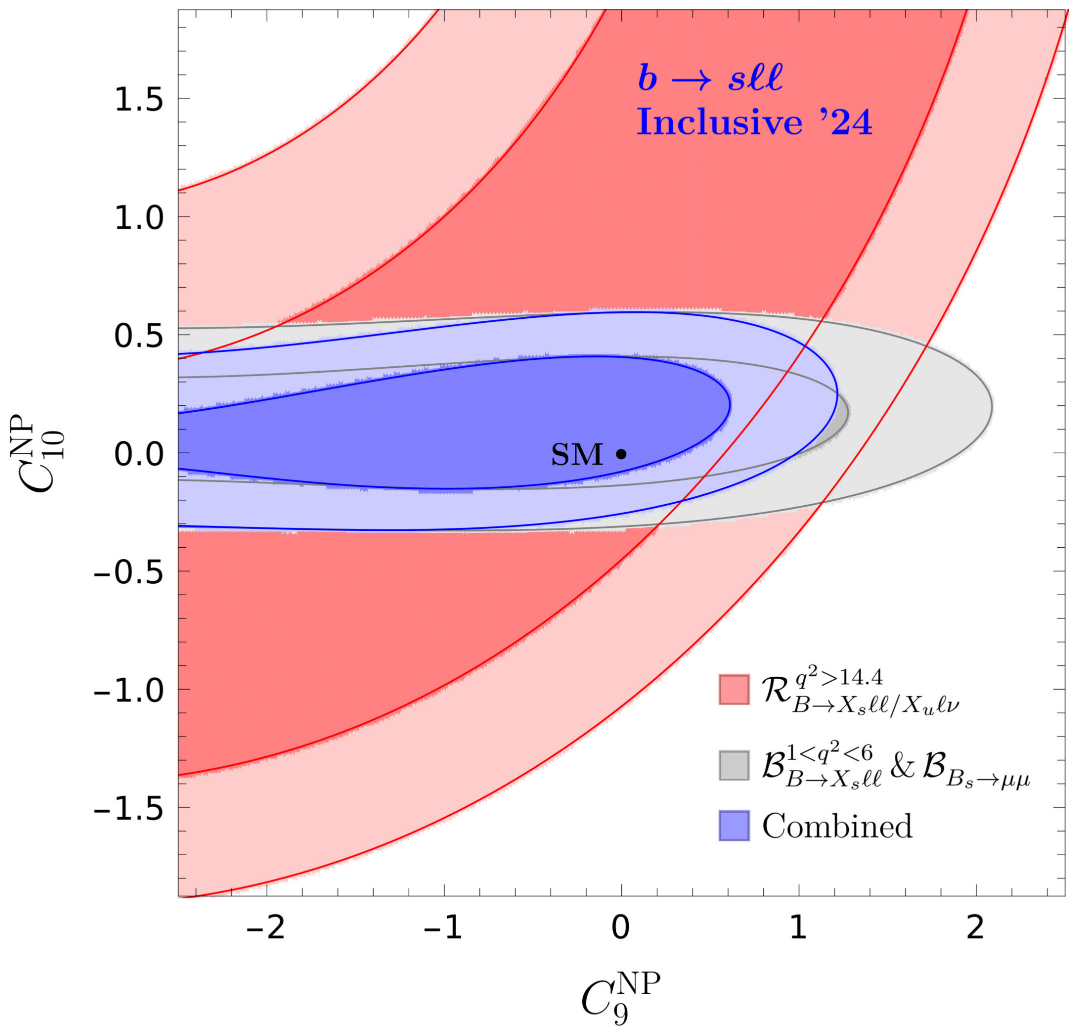

projection centered on SM

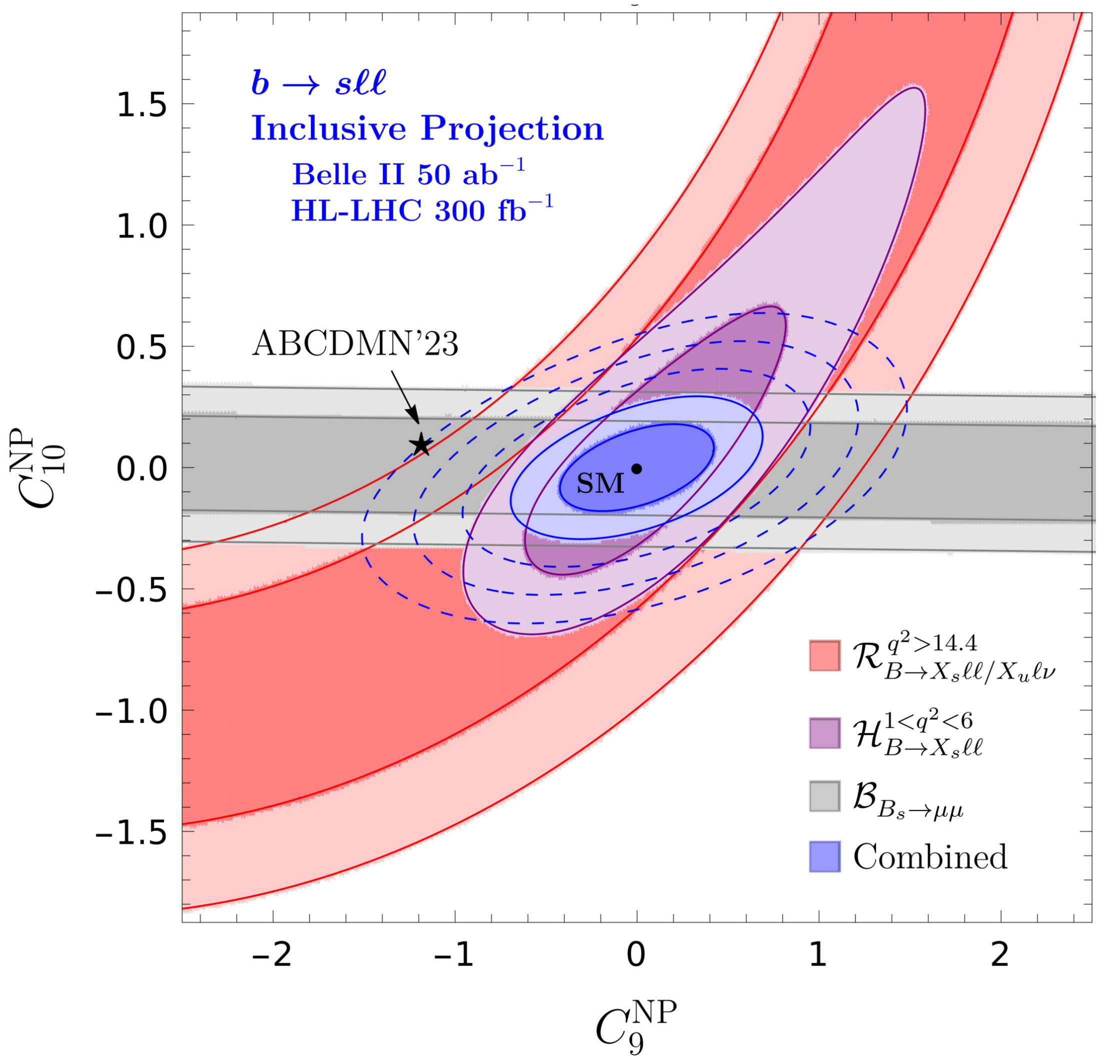

Future colliders

Azatov et al., 2205.13552

Collider	C.o.m. Energy	Luminosity	Label
LHC Run-2	13 TeV	140 fb^{-1}	LHC
HL-LHC	14 TeV	6 ab^{-1}	HL-LHC
FCC-hh	100 TeV	30 ab^{-1}	FCC-hh
Muon Collider	3 TeV	1 ab^{-1}	MuC3
Muon Collider	10 TeV	10 ab^{-1}	MuC10
Muon Collider	14 TeV	20 ab^{-1}	MuC14

$$[C_{lq}^{(1)}]_{22ij} = C_{lq}^{(1)}\delta_{ij} \text{ and } [C_{lq}^{(3)}]_{22ij} = C_{lq}^{(3)}\delta_{ij}$$

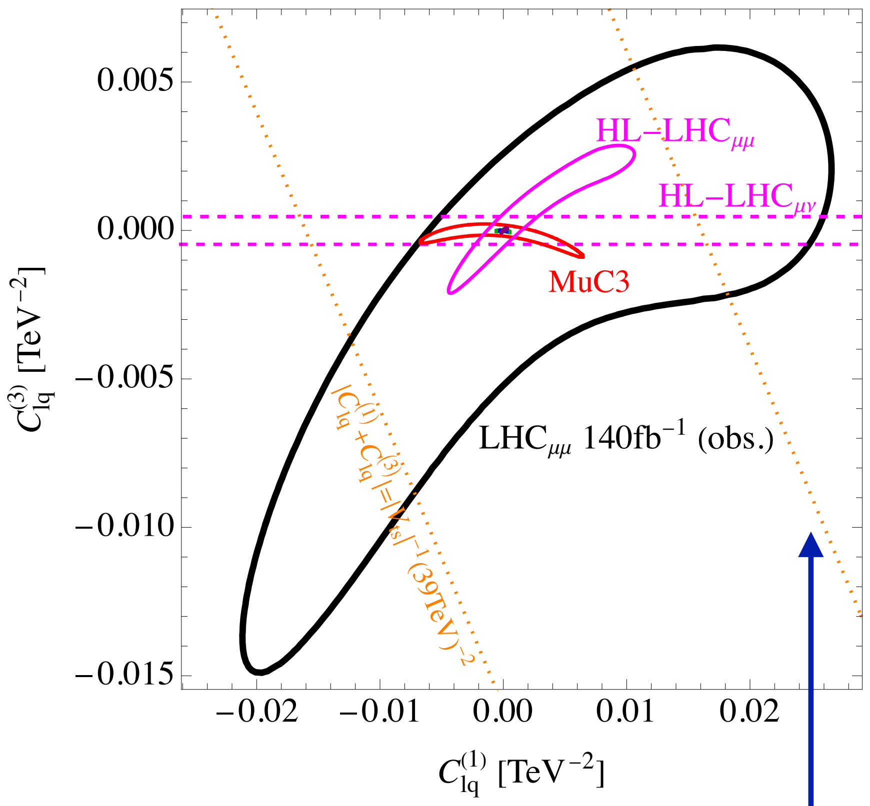

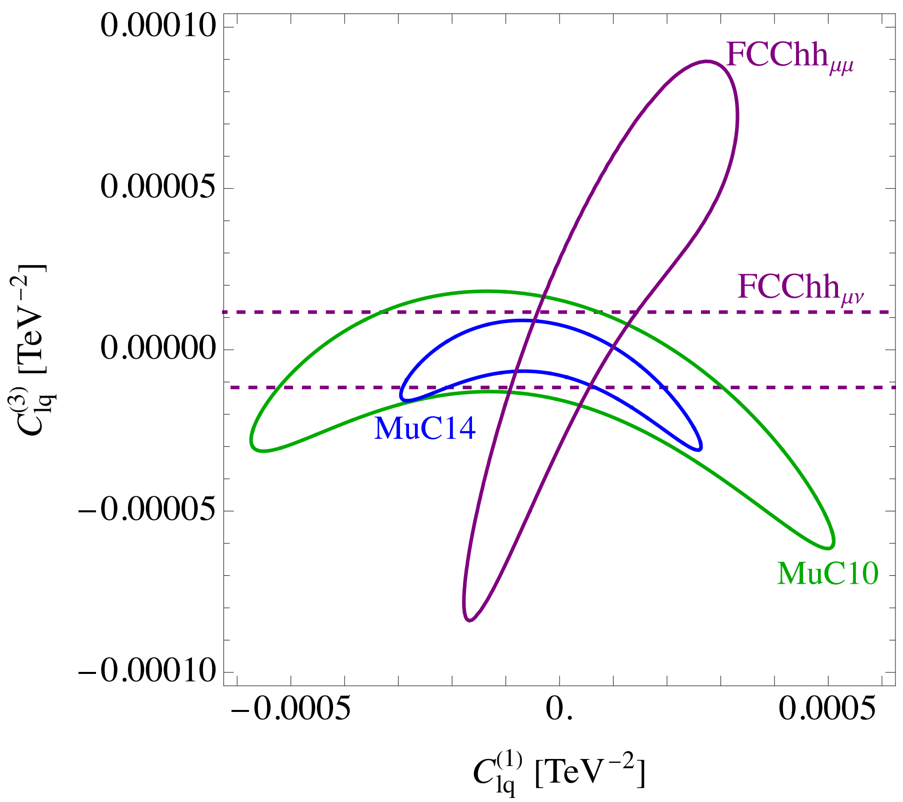

$$|C_{lq}^{(1)} + C_{lq}^{(3)}| = |V_{ts}^{-1}|\,(39\mathrm{TeV})^{-2}$$

Altmannshofer et al., 2306.15017

10 TeV muon collider (1 ab^{-1})

$$\mu^+\mu^- \to b\,s$$

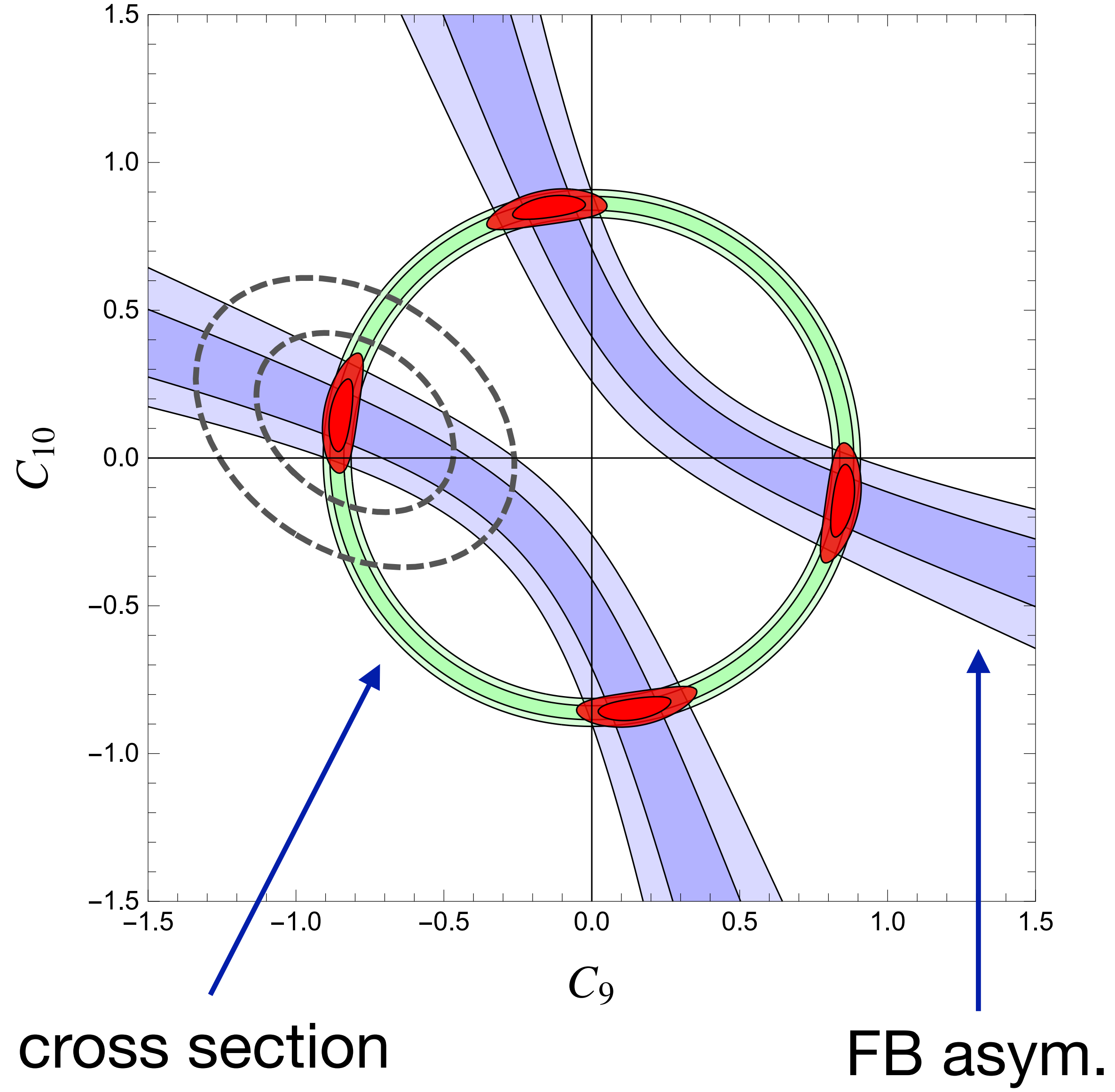

Summary

- ✦ Significant progress have been made in understanding charm loop both experimentally and theoretically.
  - ▸ Two LHCb results obtained with different models are compatible with each other.
  - ▸ Further improvements in theoretical calc's are challenging.
- ✦ LFU NP is favored by data, in contrast to LFUV NP, which had been studied to explain previous data of $R_{K(*)}$.
- ✦ Further experimental tests for anomalies are anticipated from Belle II, LHCb and other on-going experiments as well as future colliders.